Environmental Research Program

1994 Annual Report

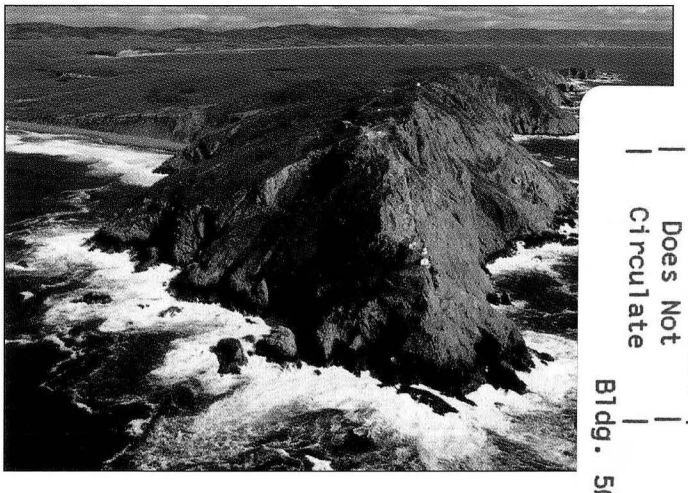

Energy & Environment Division
Lawrence Berkeley Laboratory
UNIVERSITY OF CALIFORNIA

LBL-36550
UC-350
April 1995

Available to DOE and DOE Contractors from
Office of Scientific and Technical Information
P.O. Box 62, Oak Ridge, TN 37831
Prices available from (615) 576-8401

Available to the public from
National Technical Information Service
U.S. Department of Commerce
5285 Port Royal Road, Springfield, VA 22161

Prepared for the U.S. Department of Energy under Contract No. DE-AC03-76SF00098

DISCLAIMER

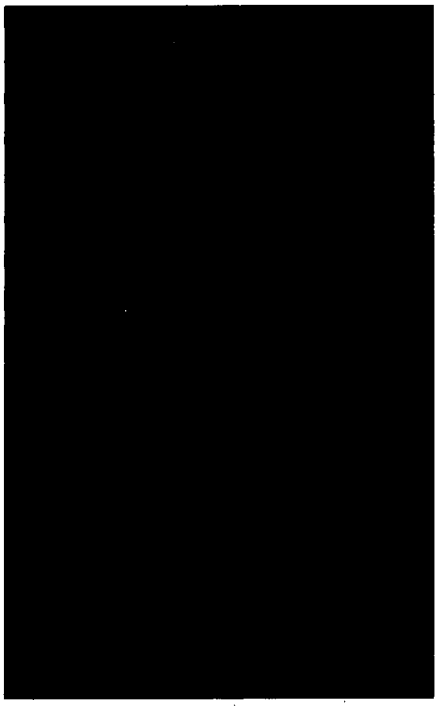

Environmental Research Program 1994 Annual Report

Nancy J. Brown, Program Head

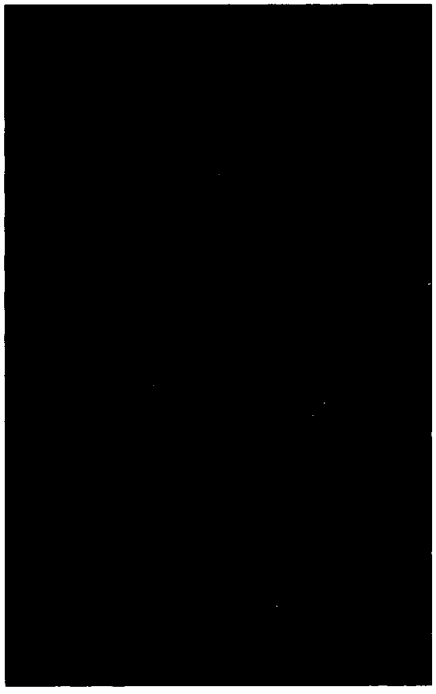

Energy & Environment Division
Lawrence Berkeley Laboratory
University of California
Berkeley, California 94720
(510) 486-5001

Report No. LBL-36550

Contents

Introduction

The objective of the Environmental Research Program is to enhance the understanding of, and mitigate the effects of pollutants on health, ecological systems, global and regional climate, and air quality. The program is multi-disciplinary and includes fundamental research and development in efficient and environmentally-benign combustion, pollutant abatement and destruction, and novel methods of detection and analysis of criteria and non-criteria pollutants. This diverse group conducts investigations in combustion, atmospheric and marine processes, flue-gas chemistry, and ecological systems.

Combustion chemistry research emphasizes modeling at microscopic and macroscopic scales. At the microscopic scale, functional sensitivity analysis is used to explore the nature of the potential-to-dynamics relationships for reacting systems. At the macroscopic level, combustion processes are modelled using chemical mechanisms at the appropriate level of detail dictated by the requirements of predicting particular aspects of combustion behavior. Parallel computing has facilitated the efforts to use detailed chemistry in models of turbulent reacting flow to predict minor species concentrations.

Investigations in turbulent combustion have resulted in development of a laboratory burner that produces very intense turbulent flames. It can be used for fundamental research of turbulence-flame interactions under the conditions encountered in most practical devices. It is also ideal for future work on ignition and extinction phenomena. With the award of a DOE Energy Research Laboratory Technology Transfer Co-Operative Research and Development Agreement with Teledyne-Laars in Moorpark, California, a program was initiated to commercialize the weak-swirl burner for use in small to medium water heaters. The focus is to develop a production prototype operating at 10 to 50 kW. Progress in the investigation of flame-gravity coupling includes completing a series of microgravity experiments on board a Learjet. The results help to identify the gravitational influences on flame propagation.

In the past year, the Flue Gas Chemistry Group has focused on controlling and converting atmospheric and aqueous pollutants. They have continued to develop techniques for converting NO, SO_2, and CO_2, which are pollutants from energy generation. The simultaneous removal of SO_2 and NO from flue gas by using an aqueous mixture of limestone and an iron compound has been successfully demonstrated on a bench-scale scrubber. In addition, a catalyst which is capable of converting SO_2 to elemental sulfur in the presence of moisture has been developed. A new, phosphorus-based process called POZONE has been developed and applied to help paper manufacturers bleach white paper without creating wastewater containing hazardous chlorinated-organic compounds.

In research exploring thermal destruction of toxic compounds, metal atoms and compounds have been detected in high temperature combustion exhausts using a variation of excimer laser fragmentation fluorescence spectroscopy (ELFFS) and a patent application for this method has been submitted. A CRADA with Thermatrix Inc. has been initiated to study and measure the destruction of chlorinated hydrocarbons in a commercial packed bed reactor. A detailed reaction mechanism has been developed for the high temperature destruction of 1,1,1-trichloroethane.

The Atmospheric Processes Group has developed and validated a methodology to quantify the contributions of sulfate, seasalt, and organic components to cloud condensation nuclei number concentrations. They have found that at Point Reyes, California, the contributions of organic and sulfate aerosols to CCN are variable, ranging from ~20 to ~65% for sulfate and ~5 to ~80% for organic aerosol.

Particles in the atmosphere affect visibility, cloud formation, radiative transfer, and the heating and cooling of the earth. Researchers are investigating optical properties of the marine boundary layer (MBL) to study visibility and radiant transfer near the ocean surface. Mie scattering models were developed to calculate the polarization properties of light scattered from combinations of particles of varying size distribution and composition. Scattering predicted from aerosols whose size distributions and composition have been measured in the MBL were found to differ from the scattering predicted from marine aerosols whose size distributions are computed using aerosol formation models. Scattering induced by a sea salt component caused significantly different polarization from that predicted for soot components. These calculations suggest that the polarization of light in the marine atmosphere is variable, that predictions using common models of size distributions may need modification, and that measurement of the polarization of light in the marine environment would be useful in determining the aerosol composition.

Programs in ecological systems are diverse, ranging from genetic ecotoxicology to studies of global climate change. Researchers in the Genetic Ecotoxicology Research Laboratory have investigated the relationship between genotoxic response and reproductive success in aquatic organisms. Specifically, they established this relationship for two animal models—sea urchins and nematodes. They developed an assay using sea urchins to evaluate effects of exposure to UV-B - the first animal model to evaluate the genotoxic effects of Antarctic ozone depletion. They have established that ambient levels of UV-A and UV-B have significant effects on sea urchin embryos in Antarctica, even after peak ozone depletion. LBL ecotoxicology scientists have also performed an important role in establishing broad priorities for the field of ecotoxicology. The group enjoyed organizing the Napa Conference on Genetic toxicology that was funded by the National Institute of Health.

Methane, an important carbon sink and greenhouse gas, may be sequestered in hydrates (clathrates). The conditions of methane clathrate formation have been measured in sea water (salinity = 35 parts per thousand) and in solutions represen-

tative of anoxic marine pore waters. Methane-hydrate stability curves for all solutions can be successfully and simply predicted to within analytical precision for any solution. Using dissolved ion concentrations for pore waters in and near hydrated sediment, it was found that methane hydrate is slightly less stable in most pore waters than in sea water.

In response to a request from the Program for Ecosystem Research in the Office of Health and Environmental Research of the U.S. Department of Energy (DOE), new innovative approaches and strategies to identify and quantify the vulnerability of ecological systems to atmospheric and climatic changes were suggested. Unique applicable scientific capabilities at LBL were identified. The approaches included 1) Adaptive and Molecular Genetic Responses: Studies of the Interactions of Ecosystems with Climatic and Atmospheric Changes; 2) Anoxic Regimes, Environmental Stress, and Greenhouse Gas Biogenesis; 3) Integrated Paleoclimatic and Paleoecological Study of a Western Delta Watershed; 4) Interactions Between Biogenic Aerosols and Climate; and 5) International Assessment of Ecological Consequences of Climate Change on Forest Sectors.

Program scientists have worked with other investigators within the Energy and Environment, Earth Sciences, Life Sciences, and Information and Computing Sciences Division on the SELECT project. The goal of the SELECT project is to design and develop a distributed, object-oriented computer architecture to integrate, analyze, and present environmental information to help managers select cost-effective environmental remediation that maximizes health-risk reduction while minimizing costs. A salient feature of the architecture design will be the incorporation of state-of-the-art scientific advances in site characterization, subsurface and atmospheric transport processes, exposure pathway analyses, and health-hazard assessment, as well as financial analyses of environmental remediation. Comparison of estimated cancer risks from background exposures (*e.g.*, from indoor sources or natural chemicals in the diet) with potential exposures from the contaminant site are also being incorporated.

Program Staff

Nancy J. Brown*, *Program Leader*

Lisa Alvarez-Cohen
Susan Anderson
Frank Asaro
Benoit Bedat†
Kimberly Brouwer‡
Robert Buchanan
Steven Buckley†
Johnny Chang
Shih-Ger Chang*
Jyh-Yuan Chen
Robert Cheng
Craig Corrigan
Gerald Dickens†
Robert Dibble
Stephan Engleman†
Drazen Fabris
Carlos Fernandez-Pello
Charles Fleischmann
Ian Fry
Jeronimo Garay
Stephen Gehlbach‡
Robert Giauque
Gloria Gill
Ralph Grief
Robert A. Harley
John Harte
Erika Hoffman
Jennifer Hoffman
Jack Hollander
Kenneth Hom
Gary Hubbard
James Hunt
Mary Hunt
John Jelinski
David Jenkins
Yun Jin†
Revital Katznelson
Jay Keasling
Peter Kettler
John Knezovich†
Tatsuya Kodama†
Catherine Koshland
Gerhard Lammel†
Shuncheng Lee
Terrance Leighton
Guoping Li
He Li†
David Littlejohn
Donald Lucas
Robert Macey
John Maguire
Samuel Markowitz
Rolf Mehlhorn
Katherine Moore
Tihomir Novakov*
Antoni Oppenheim
Lester Packer
Patrick Pagni
Joyce Penner†
Robert Risebrough
Carlos Rivera-Carpio
C. Fredrick Rogers†
Walter Sadinski
Robert Sawyer
Richard Schmidt
Ian Shepherd
Yao Shi†
Martyn Smith
Fred Stross
Lawrence Talbot
Chang-Lin Tien
Shu-Mei Wang†
R. Brady Williamson
Michelle Wilson‡
Linda Wroth
Yi-Ran Wu
Lin Bin Xu
Ya-Hui Zhuang†

*Group Leader
†Participating Guest
‡Student Assistant

Flue Gas Chemistry

Bench Scale Tests of Fe^{2+}(DMPS) Solutions for the Removal of NO Gas

Y. Shi and S.G. Chang

Fe^{2+}(DMPS) solutions have been demonstrated to possess several suitable chemical properties for the absorption of NO from flue gas. These properties include a high NO absorption capacity, more resistance to the oxidation by oxygen, and the ability to form a stable iron nitrosyl compound. The absorbed NO can be converted to ammonia by both electrical or chemical reduction methods. In the last year, we have conducted laboratory experiments to obtain data for use in the prediction of NO removal efficiency in a commercial-scale scrubber. The removal efficiency of NO in a scrubber depends not only on chemical reaction rates but also on the mass transfer rate. We have performed experiments with a stirred reactor to determine the chemical reaction rate of NO with Fe^{2+}(DMPS) solutions. In addition, we have carried out tests on a bench-scale scrubber to determine the mass transfer contribution and the parameters that affect the NO removal efficiency. Furthermore, we have made an attempt to predict the performance on a full-scale limestone spray absorber.

A double stirred reactor with a plain gas-liquid interface was used to measure the absorption rate of NO in Fe^{2+}(DMPS) solutions. The liquid-side mass transfer coefficient for the system was determined by measuring the rate of absorption (as a function of liquid stirring speed) of carbon dioxide into water at 25°C. The gas-side mass transfer coefficient was determined from the absorption (as a function of the gas stirring speed) of sulfur dioxide into a sodium hydroxide solution. These values were used in analyzing the transfer of NO into solutions of Fe^{2+}(DMPS). Under the conditions of the experiment, the concentration of Fe^{2+}(DMPS) in the solutions was much greater than the concentration of NO at the interface and the process simplifies to pseudo-first order conditions. The results indicated that the absorption rate was nearly proportional to the partial pressure of NO. The reaction rate constant was 1×10^7 l/mol-sec at 55°C.

The bench-scale tests were conducted with a 4"-diameter turbulent contact absorber (TCA).

TCA is a gas absorber containing a bed of low density spheres fluidized by upward flowing gas while scrubbing liquors are pouring downward. The spheres are hollow plastic balls that have densities below that of water. Tests with a TCA would allow a more accurate measurement of gas-liquid interfacial area per unit volume of contact zone because of less wall effect compared with a regular spray absorber. In addition, when compared with a packed bed reactor, plugging is less likely to occur in the fluidized bed. The results on a TCA show that the removal efficiency of NO increases along with an increase of L/G (the flow rate ratio of scrubbing liquids to flue gas in gpm/1000 acfm). With a Fe^{2+}(DMPS) concentration of 47 mM, the removal efficiency was 63% and 53% at an L/G of 118 and 70 respectively. In addition, the results indicated that the removal efficiency of NO is independent of NO concentration in flue gas.

Based on a mathematical model and on the TCA results, we have made an attempt to predict the performance on a full-scale limestone spray scrubber. The number of transfer units would be 0.5 which corresponds to a NO removal efficiency of 40%, assuming the height of a spray absorber to be 60 ft, a flue gas superficial velocity of 10 ft/s, and an average spray droplet diameter of 2 mm. If the diameter of droplets could be reduced from 2 mm to 1.5 mm while maintaining all other parameters, the number of transfer units would increase to 1.17 which corresponds to a NO removal efficiency of 69% . Further reduction of the diameter of droplets would substantially increase the removal efficiency of NO.

We are currently working on a new regeneration method for the Fe^{2+}(DMPS). We will conduct integrated tests on a bench-scale limestone system.

POZONE Process for the Bleaching of Pulp

S.M. Wang, D. Littlejohn, and S.G. Chang

Current methods for bleaching paper pulp rely heavily on chlorine and chlorine-containing compounds. While these processes are effective, they can produce dioxin and other chlorinated compounds. There are increasingly stringent regulations on release of chlorinated hydrocarbons in wastewater and to the air. Alternatives to chlorine-based bleaching processes are needed. We had previously utilized yellow phosphorus as a source of ozone in flue gas scrubbing systems and in destruction of hazardous organic compounds. We have found that it is also effective in bleaching and delignifying paper pulp.

This research was conducted to determine the effectiveness of yellow phosphorus in paper pulp processing. A brightness measurement system was set up to determine the change in brightness of the pulp during treatment. Initial studies investigated the bleaching of low consistency pulp, using 2% pulp in water with P_4 at 60°C. The mixture was stirred and air was bubbled through it. Pulp treated by this process (POZONE) showed some increase in brightness, although the increase was small. We believe that this was due to poor contact between the phosphorus and air.

From the information gained in the early studies, an improved reaction system was developed. The pulp was first

acidified and water was removed to 50% consistency. The pulp was then suspended above a spray/aeration contact system for the water-phosphorus mixture. The gas stream from this system carried the ozone generated to the suspended pulp. This process achieved substantial brightness gains in the pulps tested. The changes achieved are listed below.

In one step, the phosphorus treatment generated brightnesses comparable to those obtained commercially using chlorine, caustic, and hypochlorite treatment steps. This indicates that this is a very promising concept.

After discussions with pulp companies, we believe the POZONE treatment of pulp would be best performed following the oxygen delignification step and before the final hydrogen peroxide bleaching step. We have obtained oxygen delignified pulp from several pulp companies. We are using these pulps to optimize the increase in brightness in the minimum amount of time.

In addition to the brightness of pulp, we are studying the effect on the fiber strength (viscosity) and lignin content (kappa number) of pulp subject to the POZONE treatment.

We are continuing our development of the use of phosphorus in the bleaching and processing of paper pulp. We are in contact with several pulp companies on how to best apply this promising new technology.

Sample	Initial Brightness	Final Brightness
pulp L	44	81
pulp G-P	52	77
pulp L-P	46	70
pulp W	28	72

POZONE Process for the Destruction of TCE

S.M. Wang and S.G. Chang

In recent years, we have been studying the effectiveness of yellow phosphorus in destroying toxic organic compounds. Trichloroethylene (TCE) is a halogenated hydrocarbon that is widely used in industrial applications. In the past, there have been TCE leaks and spills that have contaminated soil and groundwater. Technologies are being developed for extraction of TCE from contaminated sites, but disposal of TCE is still difficult.

We report here our studies of the destruction of TCE using yellow phosphorus in the POZONE process and using ozone alone. Yellow phosphorus reacts with oxygen to produce oxygen atoms and phosphorus-oxygen compounds. These products interact with molecular oxygen and water to generate ozone and hydroxyl radicals. Ozone and hydroxyl radicals can attack TCE and break it down to innocuous organic substances.

Experiments were conducted by bubbling nitrogen through TCE in a water bath to generate a gas mixture containing TCE. Ozone was generated by flowing oxygen through a corona discharge-type ozone generator. The oxygen-ozone mixture was flowed into the nitrogen-TCE mixture, and the gases were flowed through a heated reactor. The gases were then flowed through a sodium hydroxide solution. Samples of the gas stream could be collected before or after the reactor and analyzed by gas chromatography for TCE and CO_2. The sodium hydroxide solution was analyzed for organic compounds collected from the gas stream by ion chromatography. In the phosphorus experiments, air was added to the nitrogen-TCE mixture and flowed through a reactor through which a phosphorus-water mixture was sprayed and recirculated in countercurrent fashion. The gases leaving the reactor were again trapped with a sodium hydroxide solution. Reactant and product analyses were conducted in the same manner as the ozone experiments. Some experiments were also conducted using hydrogen peroxide in conjunction with yellow phosphorus.

The products generated by the oxidation process include CO_2, dichloroacetic acid, formic acid, glyoxylic acid, and chloride ion. Yellow phosphorus was converted to phosphate and phosphite ions.

Improved TCE removal by ozone was observed as the reactor temperature was increased. Longer contact time improved the destruction of TCE by both the ozone and POZONE processes. TCE removals of 70% to in excess of 90% were observed. The ratio of reactant to TCE had more effect on TCE removal in the ozone process than in the POZONE process. Addition of H_2O_2 to the POZONE system did not improve TCE removal or conversion to CO_2. Lower TCE removal was obtained when the TCE concentration was increased. The POZONE process appears to be a promising method for TCE destruction, and we plan to continue to develop the process to optimal conversion.

Effect of Water on the Catalytic Reduction of Sulfur Dioxide

Y. Jin and S.G. Chang

Sulfur dioxide is a major pollutant in power plant flue gases. Processes are currently under development to extract and concentrate the SO_2 from the flue gas. It is advantageous to convert the extracted sulfur dioxide to elemental sulfur, since the element is in greater commercial demand. An inexpensive, efficient method of reduction of SO_2 to elemental sulfur is needed. Earlier, we reported the development of an efficient catalyst, Cat S, to promote the reduction of sulfur dioxide with synthesis gas and methane. The catalyst is composed of several metal oxides on a γ-alumina support. The overall reaction can be written as:

$$2\,SO_2 + 3\,H_2 + CO \rightarrow S_2 + CO_2 + 3\,H_2O \quad (1)$$

There are a number of reactions that can occur on the catalyst, some of which produce undesirable products such as hydrogen sulfide, carbonyl sulfide, and carbon disulfide. The catalyst has shown high selectivity for the desired products over a wide range of operating conditions.

Previously, the catalyst had been studied only using pure reactant gases. In industrial situations, however, a number of contaminants may be present which could interfere with the operation of the catalyst. One common contaminant is water, which may be present as the result of an aqueous-based sulfur dioxide extraction process. We have conducted a number of studies on the effect of water vapor on the operation of the catalyst. Water vapor was added to a flow of sulfur dioxide, carbon monoxide, and hydrogen to generate a concentration of 15% H_2O. The mixture was flowed over the catalyst bed at a range of conditions, and the yields of elemental sulfur, hydrogen sulfide, and carbonyl sulfide were measured.

At the lowest temperature, 340°C, the presence of water caused significantly poorer yields of elemental sulfur and carbon, and increased the production of COS. However, the effect of water diminished with increasing temperature, and at 440°C and above, there were only minimal differences between the yields with water and without water. The conversion as a function of the molar ratio R = [(CO + 3 H_2)/SO_2] was studied in the presence of water vapor. It was found that the highest yield of elemental sulfur (97.1%) was obtained at R = 2.2, whereas without water, the maximum sulfur yield was 94.4% at R = 2.0. This can be understood from the effect of water on the following equilibria:

$$SO_2 + 2\,H_2 \leftrightarrow 0.5\,S_2 + 2\,H_2O \quad (2)$$

$$SO_2 + 2\,CO \leftrightarrow 0.5\,S_2 + 2\,CO_2 \quad (3)$$

$$SO_2 + 2\,COS \leftrightarrow 2\,CO_2 + 1.5\,S_2 \quad (4)$$

$$CO + 0.5\,S_2 \leftrightarrow COS \quad (5)$$

Water drives reaction (2) to the left, resulting in a corresponding shift of reactions (3) and (4) to the right. The higher value of R can be attributed to reaction (5). The additional COS formed is consumed in reaction (4).

From these studies, we conclude that the presence of water in the reaction mixture will not have a significant deleterious effect on the conversion of sulfur dioxide to elemental sulfur. The effects of water are most pronounced at lower temperatures. The optimal conversion conditions obtained with water were fairly similar to those in the absence of water, and water did not have a significant effect on yields at these conditions.

Decomposition of CO_2 to Carbon Using Ferrites

T. Kodama and S.G. Chang

There is considerable interest in methods to convert carbon dioxide to other compounds due to the rising concentrations of CO_2 in the atmosphere. Catalytic methods of carbon dioxide conversion have been reported, but many processes require high temperatures and exhibit relatively low selectivity. We have been investigating the decomposition of CO_2 on modified ferrites at the relatively low temperature of 300°C, with promising results.

Previously, magnetite had been found to be effective in the reduction of CO_2 to carbon. Ferrites belong to the same spinel-type structure as magnetite and are promising candidates for efficient reduction of carbon dioxide. Ferrites can be prepared with divalent transition metal ions substituted for iron. Nickel(II)- and cobalt(II)-bearing ferrites were prepared by the air oxidation of a hydroxide suspension of ferrous sulfate and either nickel or cobalt sulfate. After preparation of the modified ferrite solid, it was characterized by x-ray diffractometry and Mossbauer spectroscopy.

The ferrites were activated by flowing hydrogen over them at 300°C. The hydrogen reduced the material to create an oxygen-deficient ferrite that retained the spinel structure. Excessive reduction of magnetite by hydrogen created metallic iron. This material showed much lower reactivity to CO_2 than optimally reduced magnetite. Care was taken to avoid excessive reduction of nickel and cobalt-bearing ferrites to avoid the formation of metallic components.

The reduction of CO_2 was conducted by injecting a known amount of CO_2 into a sealed tube containing the material under test at 300°C. Gas samples were collected periodically and analyzed by gas chromatography. Both of the substituted ferrites proved to be superior to magnetite in the reduction of CO_2, and Ni(II)-bearing ferrite was substantially better than Co(II)-bearing ferrite. The lattice constant of the Ni(II)-bearing ferrite increased after reduction by hydrogen, indicating oxygen deficiency. After contact with carbon dioxide at 300°C, the lattice constant decreased. This shows that the oxygen atoms from the decomposition of CO_2 are incorporated into the oxygen-deficient lattice.

After reaction with carbon dioxide, the solid was analyzed for carbon. One analysis was conducted by dissolving the material in hydrochloric acid and filtering out the undissolved carbon. This method isolated only 51% of the carbon formed from the reduction of CO_2. However, combustion analysis of the solid yielded a carbon content close to that determined from the loss of CO_2. The difference between the methods can be attributed to the formation of two types of carbon, one in the form of isolated carbon atoms (α form) and the other existing as polymer carbon (β form), which would be separated after dissolution.

An XPS Study of Nitrogen-Sulfur Compounds

D. Littlejohn and S.G. Chang

Nitrogen-sulfur compounds form in aqueous solutions used for absorbing nitrogen oxides and sulfur dioxide from flue gas. These compounds include hydroxyimidodisulfate (HIDS), hydroxysulfamic acid (HSA), nitridotrisulfate (NTS) and imidodisulfate (IDS), as well as hydroxylamine and sulfamic acid. The oxidation states of nitrogen and sulfur in the compounds have not been well defined. We have made X-ray photoelectron spectroscopy (XPS) measurements on a number of nitrogen-sulfur oxide solids to better understand the formation and decomposition of these compounds.

Mg Kα X-radiation (1253.6 eV) was used to excite samples of the nitrogen-sulfur compounds. The N 1s and S 1s peak positions were corrected using adventitious carbon as a reference. We found that the sulfur atoms in the R-SO_3

groups of all the nitrogen-sulfur compounds have essentially the same binding energy. The value of the sulfur binding energy (168.8-169.0 eV) is about the same as sulfate ion (168.8 eV) and noticeably higher than dithionate ion (168.6 eV). This suggests that the sulfur may be assigned a formal charge of +6.

The binding energies for nitrogen in the nitrogen-sulfur compounds vary from 399.6 eV to 402 eV. The nitrogen in HIDS is substantially more reduced than nitrite ion, and the nitrogen in NTS is even more reduced. Using a +6 charge on the sulfur atoms in the compounds, we can assign formal charges of -1 for the nitrogen in HIDS and -3 for the nitrogen in NTS. The 1s binding energies of nitrogen in the hydrolysis products, HSA and IDS, are slightly more positive than those of the parent compounds. We attribute this to the presence of the hydrogen bound to the nitrogen creating a more positive environment. Hydroxylamine and sulfamic acid form a H_3N^+ structure and create a much more positive environment for the nitrogen, with N 1s binding energies of 402.0 and 401.5 eV, respectively.

HIDS is formed from nitrite ion and hydrogen sulfite ion in a two-step process with nitrososulfonate as an intermediate. In the process, the sulfur in each hydrogen sulfite ion is oxidized from +4 to +6, while the nitrogen undergoes stepwise reduction from +3 in nitrite ion to +1 in the intermediate to -1 in HIDS. From this, we estimate that the nitrogen 1s binding energy for nitrososulfonate would be about 402 eV. Earlier studies had given nitrososulfonate the formula $ONSO_3^-$, although it would be more appropriate to write it as $^-ONSO_3$.

HIDS is also formed by the reaction of ferrous nitrosyls with hydrogen sulfite ion. A complex of ferrous nitrosyl and hydrogen sulfite interacts with another ferrous nitrosyl complex, resulting in oxidation of the sulfur to +6 and reduction of the nitrogens to +1.

$$Fe^{2+}(L)(NOHSO_3)^- + Fe^{2+}(L)NO \rightarrow$$

$$\rightarrow 2\ Fe^{2+}(L) + {}^-ONSO_3 + NO^- + H^+$$

The nitrososulfonate formed can react with hydrogen sulfite to produce HIDS.

XPS on 6-coordinate metal nitrosyls has shown a linear relationship between the nitrosyl infrared band position and the nitrogen 1s binding energy. The ferrous nitrosyls used in the studies of HIDS formation have nitrosyl Raman bands in the range of 1760 - 1800 cm^{-1}, which correlate with a nitrogen 1s binding energy of about 402 eV, a value similar to that estimated for the nitrososulfonate intermediate. This implies NO^- character in the complex.

Hydrolysis of 2-Aminoethanethiolsulfate Ions

Z.B. Zheng, D. Littlejohn, Y.H. Zhuang, and S.G. Chang

Solutions with ferrous ion complexes are useful in removing nitric oxide from flue gas. Ligands with SH groups not only stabilize ferrous ions to promote the absorption of NO, but are also capable of rapidly reducing ferric ions back to ferrous ions. We have studied the use of ferrous cysteamine ($H_2NCH_2CH_2SH$) complexes for the absorption of NO from flue gas. We found that cysteamine was converted to a Bunte salt, 2-amino-ethanethiolsulfate (AETS, $H_2NCH_2CH_2SSO_3^-$). AETS was produced from the reaction of HSO_3^-/ SO_3^{2-} (formed from dissolved SO_2) with the oxidized form of cysteamine. Cysteamine can be regenerated by the hydrolysis of AETS. The kinetics of AETS hydrolysis have been studied and compared with other Bunte hydrolysis reactions.

The previously reported values of the pK_as for AETS were checked because the reported value of pK_{a1} seemed to be exceptionally high for a sulfonate compound. The value of pK_{a2} that we obtained, 9.1 ± 0.1, was in good agreement with the previously reported value of 9.15. However, we found pK_{a1} to be < -0.5, rather than 3.1. This measurement was consistent with our Raman measurements of highly acidic AETS solutions, which showed a shift in the SO_3 band to 1023 cm^{-1} from 1028 cm^{-1} in neutral solutions.

The hydrolysis was initiated by mixing a solution of AETS and HCl under nitrogen. Samples were withdrawn periodically for analysis by ion chromatography. Measurements were made over a temperature range of 35 to 90°C and hydrochloric acid concentrations from 0.9 to 5.1 M. The hydrolysis rate is very strongly dependent on acid concentration. Highly concentrated acid solutions behave as though the effective hydrogen ion concentration (H_o, the Hammett acidity function) is higher than the actual concentration. A least-squares fit to log(k) as a function of H_o yielded slopes of 1.01 and 1.04 at 75° and 85°C, respectively, indicating a first order dependence on effective acid concentration.

Bunte salt hydrolysis reactions generally proceed by an A-1 mechanism, in which the function of the electrophile (H^+) is to convert one of the partners in the S-S bond into a much better leaving group. $H_3N^+CH_2CH_2SH$ is a much better leaving group than $H_3N^+CH_2CH_2S^-$. If the value of pK_{a1} for AETS had been 3.1, the observed acid dependence of the hydrolysis would have been difficult to reconcile with this mechanism. However, since pK_{a1} < -0.5, our results are consistent with the hydrolysis proceeding by an A-1 mechanism.

The k(obs) values were corrected for first order dependence on H^+_{eff} and AETS.

$$k\ (corr) = k(obs) / [AETS]\ [H^+_{eff}]$$

From a plot of k(corr) vs. 1/T, we derive values of A = 9.0 x 10^{12} L mol/s and E_a = 115.9 kJ/mol for the equation $k = A \exp(-E_a/RT)$. The values of the rate of AETS hydrolysis can be calculated to determine the time needed to regenerate a cysteamine solution from AETS. The acid hydrolysis of compounds with a Bunte salt structure provides an alternative regeneration method to the hydrosulfide (HS^-) treatment used to regenerate cysteine sulfonate and glutathione sulfonate. It avoids problems with the precipitation of metal ions as sulfides and other side reactions of hydrosulfide ions.

Combustion

Thermal Destruction of Toxic Compounds

D. Lucas, R.F. Sawyer, C.P. Koshland, P. Eibeck, C. McEnally, M. Thomson, S. Lee, B. S. Higgins, and S.G. Buckley

We have been studying how chemicals, especially chlorinated hydrocarbons (CHCs) and metals, react when they are heated. The thermal treatment of such compounds is used in a variety of processes, including incineration, remediation, oil and gas processing, and chemical production. The goals of our research are to gain a fundamental understanding of the chemical processes that occur when chlorinated hydrocarbons are destroyed thermally, study new ways to enhance the destruction of these compounds, and to develop new diagnostic methods for the measurement of these species and their byproducts. The measurement and transformation of metals in combustion is a new area in which we have started research.

Diagnostics and Monitoring

We continue to develop non-intrusive optical diagnostics based on excimer laser fragmentation/fluorescence spectroscopy (ELFFS). Using the CCl radical as the detected fragment, we have measured chlorinated hydrocarbons at concentrations in the ppb range with a measurement time of seconds, and in a sooting flame environment.

We have expanded the ELFFS technique to the metals in combustion exhausts. The technique, illustrated in the Figure, employs a single 193 nm laser to photodissociate metal compounds into their atoms, which then emit light specific to each element. The method has sensitivities in the parts-per-billion range, requires no sample preparation or extraction, and detects virtually all compounds containing the metals.

Flow Reactor Studies

We also study the thermal destruction of chlorinated hydrocarbons in a turbulent flow reactor, with the CHCs injected as gases, liquids, or mixtures. A new vertical flow reactor, which allows for independent control of residence time, temperature, and equivalence ratio, has been designed and built. It will allow the use of advanced in situ diagnostics, including the ELFFS methods and in situ Fourier transform infrared spectroscopy. We are currently exploring the use of fuel mixtures to enhance the destruction of chlorinated hydrocarbons and reduce the toxic byproduct formation.

Thermatrix, Inc. CRADA

Thermatrix, Inc., a manufacturer of flameless packed bed thermal reactors, and LBL have joined forces through a Cooperative Research and Development Agreement (CRADA) to determine if the optical measurement techniques developed at LBL can be coupled with the commercial reactors to destroy polychlorinated biphenyls (PCBs). A Thermatrix reactor, installed at LBL, will be equipped with ports to permit optical sampling of the gas composition. The rapid feedback of the laser diagnostics will allow for testing of wide range of experimental conditions and operating parameters.

References

Buckley SG, McEnally CS, Sawyer RF, Koshland CP, Lucas D. Excimer Laser Fragmentation-Fluorescence Spectroscopy for Total Metal Emissions Monitoring. Central States Section/Combustion Institute Spring Meeting, 1994.

Lee S, Koshland CP, Sawyer RF, Lucas D. Effects of Post-Flame Fuel Injection on the Destruction of Chlorinated Hydrocarbons. *Combustion Science and Technology* (in press).

McEnally, CS. Lucas D, Koshland CP, Sawyer RF. In Situ Detection of Hazardous Waste. *25th International Symposium on Combustion* (in press).

Thomson MJ, Higgins BS, Lucas D, Koshland CP, Sawyer RF. The Mechanism of Phosgene Formation From 1,1,1-Trichloroethane. *Combustion & Flame* 1994, **98**; 350.

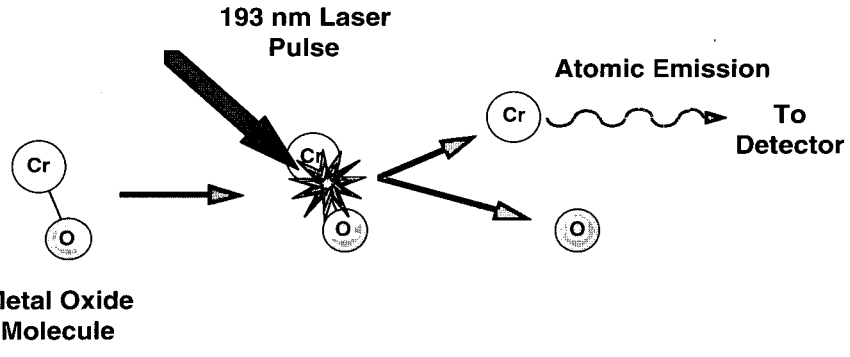

Figure. *The ELFFS technique uses light from an ArF laser to dissociate metal-containing molecules and produce metal atoms in excited electronic states. The atoms then emit light, which is used to identify and quantify the metals present in the sample.*

Combustion Fluid Mechanics

R.K. Cheng, I.G. Shepherd, B. Bedát, L. Talbot

Turbulent combustion takes place in all heat and power generating systems. Its most important role is to increase the burning rate and volumetric power density. Intense turbulence, however, also influences the chemical reaction rates of the combustion processes and has a direct effect on the formation of pollutants, ignition and extinction. Therefore, research and development of modern combustion systems for power generation, waste treatment and material synthesis must rely on a fundamental understanding of the physical effects of turbulence on combustion. Such knowledge is key to successful development of theoretical and computational models which can be used as design tools.

The overall objective of our research is to investigate the interaction and coupling between turbulence and combustion. These processes are complex and involve scalar and velocity fluctuations with time and length scales spanning several orders of magnitudes. The burner and flame geometries also have profound effects. Our approach to gain a fundamental understanding of these complex processes is by investigating laboratory flames with geometries that are designed to facilitate direct comparison with numerical modeling and theoretical analysis. These burners are also amenable to detailed interrogation by laser diagnostics and allow systematic independent variations of turbulence intensities, flow conditions and mixtures compositions.

We began by investigating flames with moderate turbulence intensity where chemical reaction rates are much faster than turbulence mixing. This type of combustion occurs in most small to medium combustion systems such as residential appliances and automobile engines at idling condition. The turbulent burning rate can be evaluated by determining how turbulence wrinkles the flame front. The flame front topology (i.e., geometry of the flame wrinkles) relates directly to turbulence scales in intensities. Recently we have extended the scope of the experiments to include flames with intense turbulence. These flames are closer to the burning conditions in larger power generating systems. Intense turbulence can affect chemical reaction rates may lead to a reduction of burning rate, intermittent flame quenching and re-ignition, and ultimately flame extinction.

Turbulent flames are affected by boundary conditions upstream and downstream of the flame. Therefore, it is important to investigate flame propagation under a variety of flow and flame geometries. We have thus far developed five laboratory flame configurations. These burners are designed to operate under a wide range of conditions so that changes in flame characteristics can be correlated to different turbulence intensities and mixture equivalence ratios. The first two configurations are simplifications of those found in many practical systems. They are a rod-stabilized v-flame propagating in turbulent flow, and a large axisymmetry Bunsen-type conical turbulent flame stabilized by a pilot flame. The next two are designed to interface with numerical models. They are planar flames stabilized in stagnation flows produced by a plate or by two opposed streams. These flames are locally normal to the approach flow and are stabilized without flow recirculation. The last configuration is a weak-swirl stabilized burner that has commercial potential in addition to fundamental significance. All of these configurations provide experimental data that can be compared with statistical one-dimensional (1-D) and deterministic two-dimensional (2-D) models, as well as three dimensional (3-D) direct numerical simulations.

Our experimental methods emphasize laser techniques with high spatial and temporal resolutions. The diagnostics for measuring statistical moments and correlations at a point include laser Doppler anemometry (LDA) for velocity and laser induced Rayleigh scattering for scalars (i.e., gas density, reaction progress variable). A simple method for determining the flame wrinkle scales is laser-induced Mie scattering from silicone-oil aerosol (MSOD). This technique is also used in conjunction with a laser sheet to render 2-D imaging of the flame wrinkle geometry at high speed (i.e., tomography). Another imaging method includes laser schlieren, a convenient means to infer overall flame behavior. The imaging systems use conventional and intensified video cameras and are interfaced with a computer controlled image processing system. With the acquisition of a dye laser system (pumped by a Nd-YAG laser), we are developing a single point and 2-D laser-induced fluorescence (LIF) technique to infer the internal flame structure. LIF is essential for us to investigate changes that occur at intense turbulence.

Flame Propagation in Intense Turbulence

As reported in 1993, we developed a burner for investigating premixed turbulent flames propagating in intense isotropic turbulence. The burner exploits the large stabilization range provided by the weak-swirl configuration. To produce intense turbulence we adopted a specialized turbulence generator. This setup produces stable flame propagation under turbulence intensities of up to 20%. The experiments were designed to investigate systematically the changes in flame structures for conditions which can be classified as wrinkled laminar flames (under moderate turbulence), corrugated flames, and flames with distributed reaction zones (under intense turbulence).

Velocity measurements by laser Doppler anemometry show that flames with intense turbulence produce very little changes in the flowfield. This is because of the high background turbulence that masks the effects due to combustion heat release. The density statistics obtained from Rayleigh scattering are quite similar to those found in flames with more moderate turbulence. These results demonstrate that point measurement techniques may not be sufficient to characterize the changes that occur under intense turbulence. As illustrated by the schlieren images of Figure 1, moderate and intense turbulent flames are drastically different. The moderate turbulent flame at left has very large wrinkles while the intense turbulence flame at right has very fine wrinkles. These fine flame wrinkles demonstrate the significant influence of small intense turbulence eddies. Quantifying their effects, however, requires more sophisticated 2-D imaging techniques. This is the motivation for acquiring the pulsed dye laser system. The high laser power available will enable the implementation of 2-D Rayleigh scattering, and 2-D LIF of radicals such as OH^+ and CH^+ to infer the changes in flame thickness and local reaction rates.

At present, the Nd-YAG laser is installed and successfully tested in a tomographic study using a gated-intensified video camera. Once the tomographic test is complete, the system will be

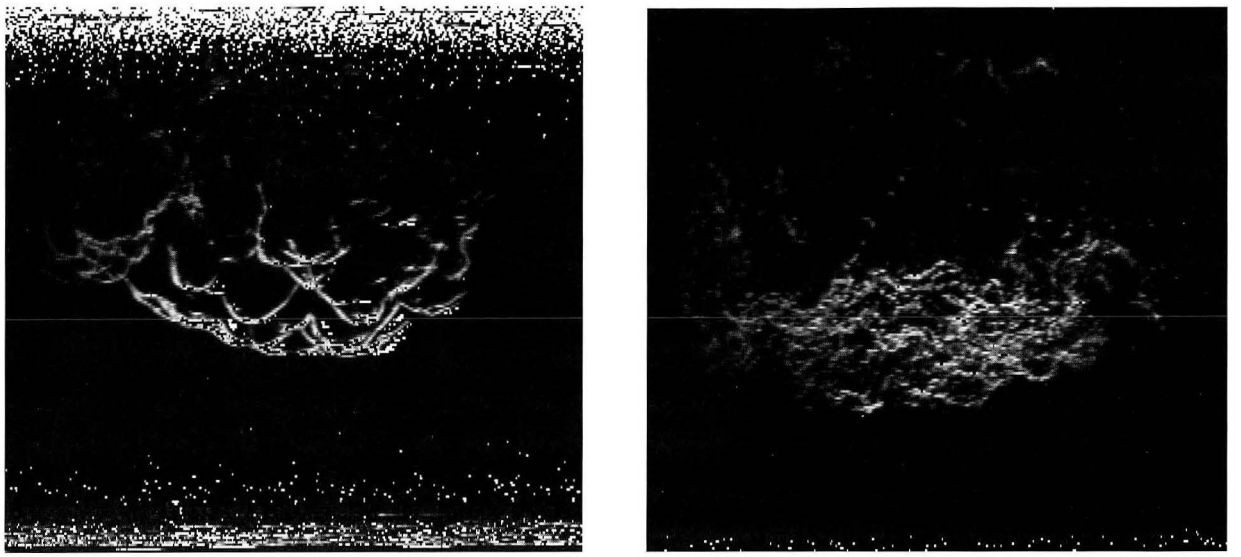

Figure 1. *Comparison of schlieren images obtained for weak-swirl stabilized flames with moderate turbulence (u′ = 0.25 m/s) and intense turbulence (u′ = 1.5 m/s).*

modified for 2-D Rayleigh. This will be followed by installing the dye laser for LIF measurements. We plan to start with the single point LIF system before progressing to 2-D.

Coupling of Premixed Flames with Gravity

Premixed turbulent flames are sensitive to conditions in their surroundings. Because of the buoyant combustion products, gravity has profound effects on many aspects of flame propagation such as burning rate, stabilization, extinction, and perhaps pollutant formation. The flame-gravity coupling processes have not been adequately addressed by laboratory experiments and are assumed to be insignificant in most combustion theories. Our approach to determine these gravitational effects is to compare the flames characteristics under normal gravity (+g), reverse gravity (-g, flame placed upside down) and microgravity (μg) conditions. The experiments are designed to show if the influence of gravitation effects diminishes with increased flow momentum. This knowledge is essential to guide and validate the development of turbulent combustion models. The μg experiments were performed at NASA Lewis Research (LeRC) Center in Cleveland Ohio. Due to the size restriction of the μg experimental facility, we use a small (25-mm diameter) burner to generate conical Bunsen type flame and rod stabilized v-flames. Laser schlieren is the primary diagnostic because the use of other methods that require high power lasers are not yet feasible. The laboratory +g and -g flames are studied in greater detail to supplement the limited amount of information obtained from μg experiments.

For the μg experiments, the burner, optics, and electronic control are fitted in a 1 m × 1 m × 0.5 m metal frame called the experimental package. The package was designed for use in 2.2-second drop tower facility at LeRC. In 1994, we converted this package for use on-board a Learjet flying in parabolic trajectories. The Learjet facility provides a much longer duration of μg (15 seconds compared to 2 seconds), and allows the experimentalist to observe the flame in μg and make adjustments when needed. Twelve successful experiments were performed yielding schlieren results of laminar and turbulent v-flames and conical flames under both μg conditions as well as enhanced gravitational condition. These results have been digitized for further analysis. We also observed flame extinction during the transition from normal to μg. This demonstrate the need to quantify the influence of gravity on flame stabilization limits.

Because the opportunities to conduct μg are rare, the study of stabilization limit can only be conducted in the laboratory. The results obtained for laminar v-flames (Figure 2) show that reversing the gravity extends the stabilization limit to much

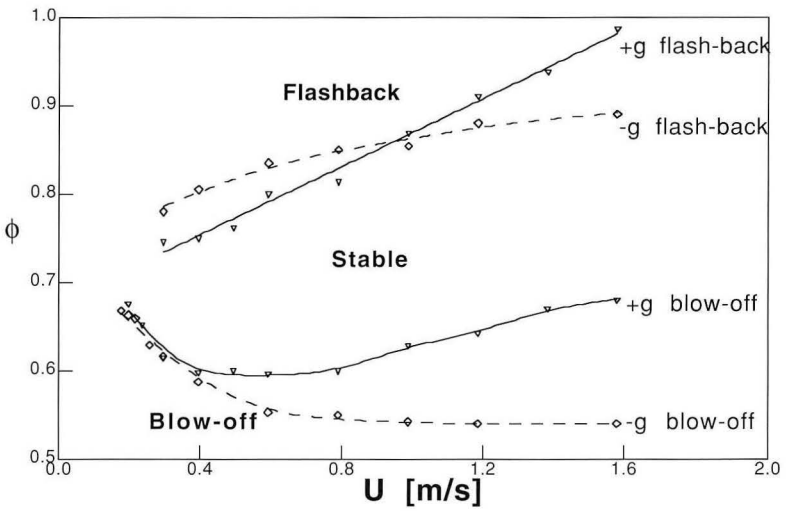

Figure 2. *The influence of gravity on the blow-off and flash-back limits of laminar v-flames. f = equivalence ratio of the premixture.*

leaner conditions. During the course of this work, we also discovered that reversed gravity can stabilize freely propagating adiabatic laminar flames. Under the appropriate conditions, flow divergence induced by the buoyant products generates the flowfield for the flame to be stabilized away from the burner rim. These flames are very stable and flat. Heat loss is minimal because the flame is not in contact with any physical surfaces. We are continuing with the characterization of the conditions under which these flames can be stabilized. We also plan to make detailed velocity and density measurements. We believe that this adiabatic flame would be of interest to fundamental studies of combustion chemistry for it does not have the upstream heat transfer problem as in the flat flame burner which is the current standard.

Hydrodynamics Effects of Premixed Flames

The mean mass burning rate or the heat release rate are parameters of primary practical importance in premixed turbulent flames. It is conventional to characterize them in terms of a turbulent burning velocity, S_T, often defined, by analogy with the laminar burning velocity S_L, as the mean velocity of the reactants upstream of a strictly one dimensional flame. Much effort has been devoted to the measurement of S_T in an attempt to correlate it with flow and flame characteristics such as velocity fluctuations, length scales, and S_L, or more broadly with dimensionless quantities such as the Reynolds and Damkohler numbers. Theoretical work, reported last year, demonstrated that the existence of flow divergence in the reactant flow can, if neglected, lead to large errors in the measured burning rate. This is true not only in configurations where flow divergence is imposed by the flow geometry (stagnation point flows) but also in, for example, open v-shaped flames where heat release at the flame front induces strain in the reactant stream.

Work on both these aspects of flow divergence in turbulent premixed flames has continued. Numerical and experimental results have been obtained which demonstrate some important hydrodynamic effects of heat release in premixed flames. The heat release at the flame front was modeled by treating the flame as a collection of volume sources. A double kernel ignition was numerically simulated and the flow induced in the reactants between the expanding kernels was investigated with special emphasis on the strain rate, i.e flow divergence, along the axis of symmetry. This was found to be sensitive to the size and shape of the flame front which demonstrates that care must be taken when interpreting experimental measurements of the burning velocity by this method.

Experiments were performed in a turbulent premixed v-shaped flame and the strain rates in the approach flow were determined tangential to the mean flame position normal to the plane of the flame and parallel to the flame stabilizer rod. Figure 3 shows the induced strain rate, i.e the velocity gradient, in the reactants in the flame zones of a series of turbulent v-shaped methane/air flames at varying equivalence ratio, ϕ. The progress variable is a non-dimensional measure of the mean density and is zero in the reactants and unity in products. As expected when the heat release increases, the flow divergence in the reactant stream rises. The neglect of this heat release induced flow divergence can lead to significant errors in measurements of the turbulent burning rate.

A series of experiments has also been performed in turbulent stagnation point flames over a range of equivalence ratios and strain rates and the affect of the flow divergence on the mass burning rate has been assessed. The results show once again that the conventional measure of the turbulent burning velocity, the reactant velocity at the cold boundary, can significantly overestimate the burning rate.

Theoretical and Numerical Analysis

Our theoretical study of premixed turbulent flames involves the development of deterministic models of turbulent combustion employing a vortex dynamics method. In contrast to the statistical modeling approach where the changes in flame turbulence are modeled and used as input parameters, the vortex dynamics model is capable of predicting these changes and other flame phenomena, in particular, the flamelet geometry. In simulating the flamelets, one needs to follow the evolution of the flamelets whose speed depends on the local curvature. The algorithms approximate the equations of motion of propagating fronts with curvature-dependent speed, which

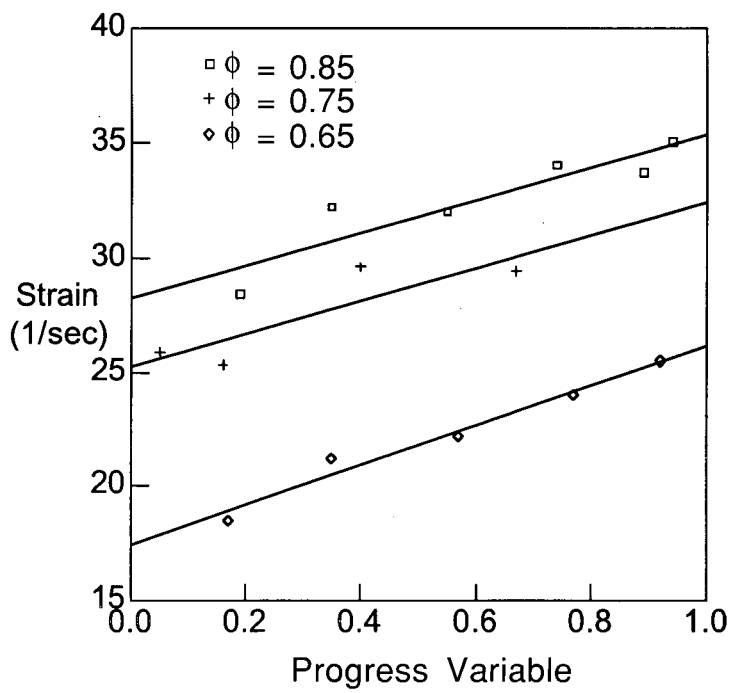

Figure 3. *Flow divergence shown here as strain induced within three methane/air turbulent v-flames. The leading edge of the flame zones (cold boundary) correspond to progress variable $\bar{c} = 0$ and the trailing edges (hot boundary) correspond to $\bar{c} = 1$.*

are called PSC schemes, for Propagation of Surfaces under Curvature. These algorithms are coupled to a vortex dynamics approach to describe both the turbulence in the oncoming stream and turbulence production by the flame itself, and a volume production model to represent combustion heat release.

We have developed a two dimensional premixed turbulent flame model which focuses on the structure of v-shaped free-burning anchored flames, including the effects of advection, volume expansion, flame generated vorticity, and curvature effects on the laminar flamelet propagation speed. Except for the restriction to two-dimensionality, this model is a fairly complete numerical representation of our previous experimental work, under the assumptions inherent in the wrinkled laminar flamelet model, where the flame can be treated as a vanishingly thin interface separating reactants and products. In accord with experimental observations, this algorithm, along with a flame anchoring scheme, predicts flame cusping for a case in which a strong vortex pair interacts with the flame front. The detailed computation velocity and scalar statistics obtained compare well with experimental results obtained previously. Comparison of the conditioned and unconditioned values of these statistics shows that the intermittency factor (i.e. the progress variable) should be considered for an accurate interpretation of experimental results a better estimation of various theoretical model predictions.

Technology Transfer

In addition to its scientific significance, the weak swirl burner is suitable for use in a variety of heating appliances. The burner supports stable combustion in very fuel lean conditions under which the emission of oxides of nitrogen NO_x is very low. The level measured in our laboratory burner operating at 30 KW is less than 10 ppm. This emission level meets or exceeds many proposed California and Federal air quality standards. With the award of a DOE Energy Research Laboratory Technology Transfer Co-operative Research And Development Agreement (ER-LTT CRADA) with Teledyne-Laars in Southern California, we have initiated a program to commercialize the weak-swirl burner for use in small to medium water heaters. The focus is to develop a production prototype operating at 14 to 20 KW. The results obtained thus far are very encouraging. We rescale the burner to a size comparable to that of current Teledyne-Laars production models. Performance tests show no undesirable effects of scaling down. The burner operates reliably when placed inside cylindrical enclosures. Unlike typical swirl burners with much stronger swirl, our burner does not produce flame vibration nor acoustical "buzzing." Some preliminary tests were performed using a heat exchanger designed for the Teledyne-Laars Telstar spa heater. The thermal efficiencies exceeded 80% even though the heat exchanger is not optimized for this burner.

Planned Activities

We plan to develop two 2-D quantitative imaging techniques for studying flame structures in intense turbulence. Planar Laser Induced Fluorescence and 2-D Rayleigh measurements will show if the reaction zone structures are altered by small scale turbulence. The experimental conditions will be extended to investigate turbulence flame quenching.

The investigation of the flame/gravity coupling will focus on the development of quantitative diagnostics suitable for use in the microgravity facilities at LeRC. Laboratory work on characterizing the effect of reversing gravitational field will continue. In particular, the free standing laminar flame produced in -g will be studied in detail so to gain an understanding of the stabilization mechanism of this very interesting flame.

The development of deterministic vortex dynamic models of premixed turbulent flames will focus on applying our model to problems of stagnation flow turbulent flames stabilized by a plate or by two opposed streams. Both configurations are axisymmetric and considered to be most suitable for investigating fundamental processes of turbulence-flame interactions.

Work planned for the CRADA with Teledyne-Laars will include construction of a testing station for the water heater. A demonstration model will be designed and used to determine the optimum conditions for high thermal efficiencies and low NO_x emissions.

Combustion Chemistry

J. Chang and N.J. Brown

Theoretical modeling of combustion involves a multilevel approach that encompasses fluid mechanical models of flames at the macroscopic level to dynamical models of chemical reactions at the microscopic level. Our research effort is focused on the fundamental chemistry aspect of combustion modeling and, in the past year, has proceeded along two fronts. The major component of our effort has been a continuation of work from previous years in attempting to elucidate the subtle relationship between inaccuracies in the potential energy surface (PES) and its effects on the molecular dynamics. We carried out this investigation using the tools of quantum functional sensitivity analysis (QFSA). In a second effort, we began a collaboration with scientists at Sandia National Laboratory, Livermore, to calculate reaction rate constants via real time Monte Carlo path integrals, in particular, employing massively-parallel computers. The details of our progress in these two fronts are described below.

The question of how errors in the PES manifest themselves in dynamical observables has been a long standing research problem in our group. Our effort in this area evolved from a series of one-dimensional studies on the collinear $H + H_2$ exchange reaction where the H-atom and the H_2 molecule are constrained to lie on a straight line. We then completed the first QFSA study of the $H + H_2$ reaction in three dimensions (3-D), that is, without imposing any artificial dimensionality constraints, but the work was applicable for only zero total angular momentum. This past year, we developed a computer code for QFSA that removes this final constraint on total angular momentum, and have used it to study how various isotopic analogs of the $H + H_2$ reaction sense their common underlying PES. We found that the $H + H_2$ and $D + H_2$ reactions sample the potential in very similar ways, but that the $H + D_2$ reaction samples the potential quite differently. In particular, for zero total angular momentum, the

reaction probability from an initial vibrational (v) and rotational (j) state v = 0, j = 0 to the rotationally-summed product vibrational manifolds v'=0 and v'=1 shows distinct resonance features for the first two reactions but no hint of any resonance for the latter H + D_2 reaction. The sensitivity maps for the two reactions containing a resonance show distinct complementary sensitivity features at the resonance energy — a change in potential which increases the reaction probability to one v' manifold will decrease the probability to the other manifold. The H + D_2 reaction, on the other hand, does not show any of this complementarity for its v'= 0 and v'= 1 sensitivities. Furthermore, for reactions containing a resonance feature, the magnitude of the sensitivities are largest at the energies near resonance.

In the course of this study, we also uncovered some remarkable sensitivity features that challenge established concepts of chemical reactivity. We found that there are large energy ranges above the reaction threshold where increasing the reaction barrier actually leads to greater reactivity! This trend exists for all three isotopes of the H + H_2 reaction. Figure 1 shows two energy slices of the total reaction probability sensitivities from the v = 0, j = 0 state at zero partial wave. The lower energy slice at E=0.82 eV shows a large region of positive sensitivity around the top of the barrier. The positive sensitivity implies that increasing the PES in this (barrier) region will increase the total reaction probability. Conversely, increasing the PES in regions of negative sensitivity (shown by dashed contour lines) will decrease the reaction probability. At higher energies, changing the barrier height has negligible effect on reactivity as the regions of large sensitivity follow a path that "cuts the corner" and is far removed from the reaction path. Figure 1b shows an energy slice illustrating this point. The significance of this result is that it forces a rethinking of how much error in the dynamics is attributable to inaccuracies in the potential above the reaction path. While it is certainly expected that the high energy dynamics will explore regions of the potential far removed from the reaction path, one might not have expected that a given error on the walls of the potential to have a larger effect on the dynamics than if the same error had been localized on the reaction path.

In our Sandia collaboration, we are investigating the feasiblity of using massively-parallel computers to evaluate real time Monte Carlo path integrals. In the past, attempts at direct evaluation of the path integrals arising from the flux-flux autocorrelation function formulation of reaction rate theory have failed because the highly oscillatory integrands precluded convergence on conventional supercomputers. We are thus querying whether or not a thousand-fold increase in computing power is sufficient to converge the path integrals. If this approach succeeds, we will have a powerful method for calculating rate constants that is applicable to a wide variety of chemical reactions. We are currently testing

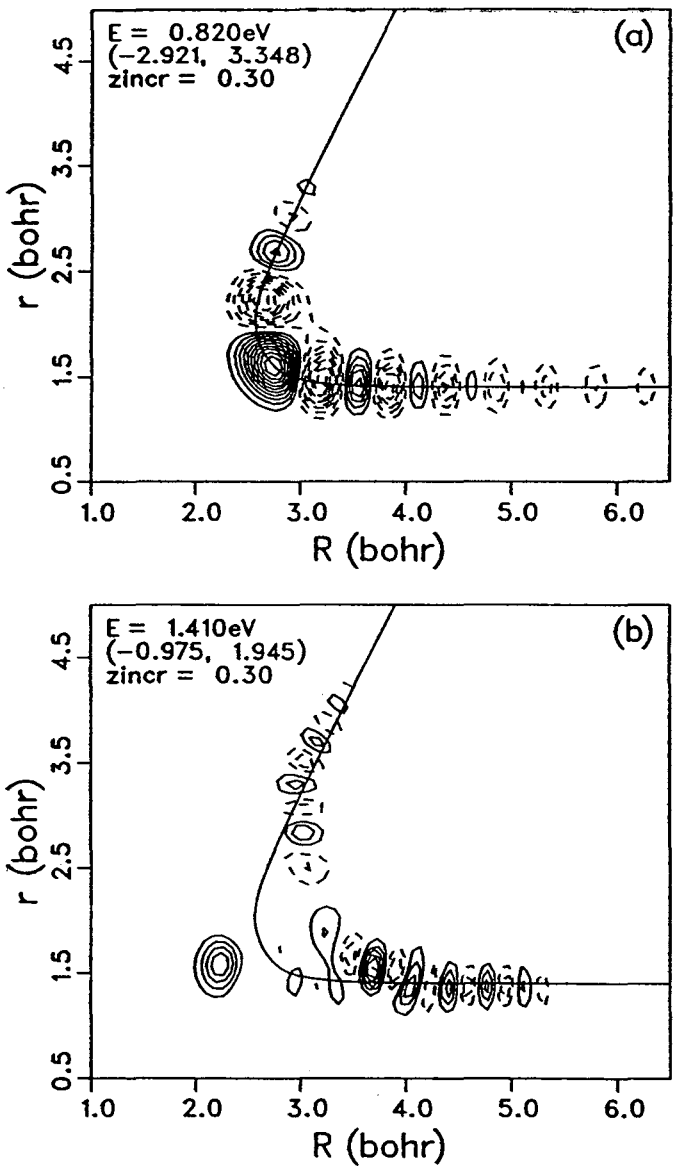

Figure 1. *Sensitivity maps for the zero partial wave total reaction probability from the initial v = 0, j= 0 state at two energies (a) E = 0.82 eV and (b) E = 1.41 eV and at a Jacobi angle of 180°. The contour values are drawn in increments of zincr shown on the plots. Positive contours are represented by solid lines and negative contours by dashed lines. The zero contour line is omitted. The numbers in parentheses represent the minimum and maximum sensitivity values on an 80 × 65 rectangular grid. All sensitivity contour values are given in units of $eV^{-1}bohr^{-6}$. The reaction path is shown on the plots by a solid heavy line.*

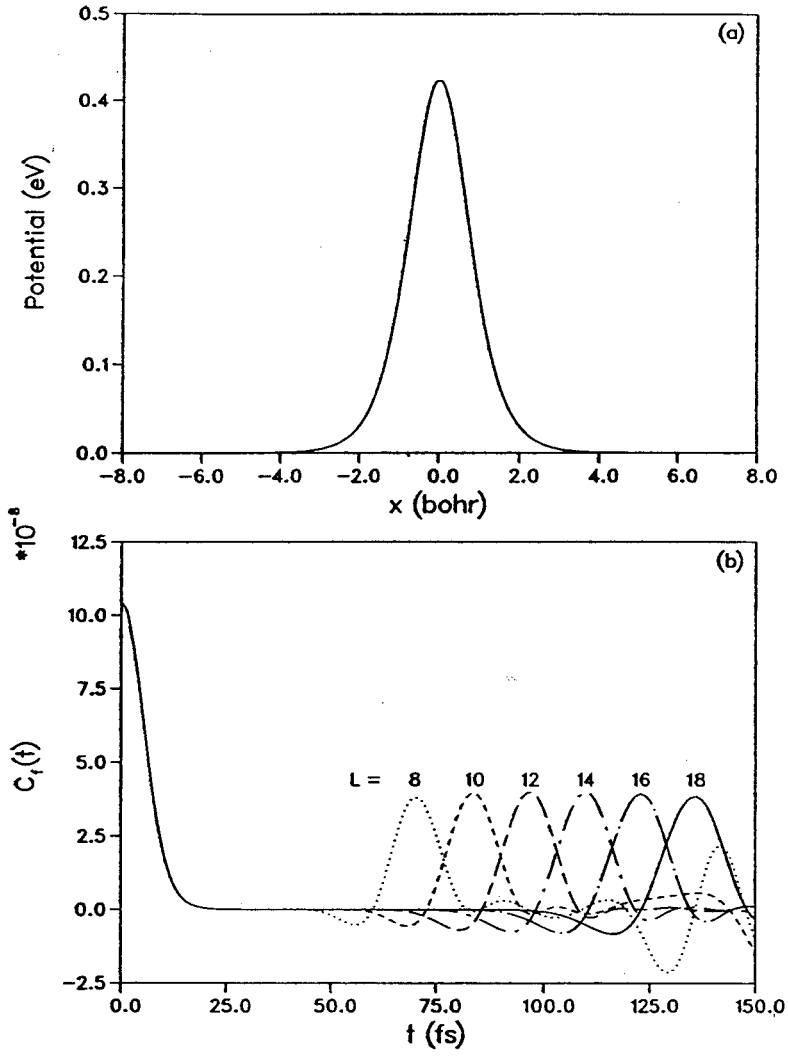

Figure 2. *(a) Eckart potential, (b) Time dependence of the flux-flux autocorrelation function for different values of the box size (L). The box sizes are in units of bohr, time in units of femtoseconds, and the autocorrelation function in units of* $(\hbar\beta)^{-2}$.

the methodology for an H-atom tunneling through a simple one-dimensional Eckart barrier. Figure 2 shows a plot of this potential along with the flux-flux autocorrelation function generated by a basis set approach. We used a finite set of Gaussian basis functions equally distributed in coordinate space. The region spanned by the basis set defines a "box" where the "walls" reflect flux after some period of time. The larger the box, the longer it takes before the artificial walls interfere with the dynamics.

For future work, we plan to extend our sensitivity analysis work to other chemical reactions. Both the $F + H_2$ and $H + O_2$ reactions are currently mired in controversy with the brunt of the blame being placed on inaccuracies in the PES. We believe that QFSA can provide feedback information to quantum chemists in their PES refinement efforts. For the rate coefficient work, there are several methods currently under investigation. The main thrust of these investigations is to eliminate the need for state-to-state reactive scattering calculations, and thus to considerably simplify the calculations without sacrificing accuracy. As the method of choice emerges, concomitant development in sensitivity analysis will be required.

References

Chang J, Brown NJ. Quantum functional sensitivity analysis for the 3-D (J = 0) H + H_2 reaction. *Int. J. Quantum Chem. Symp.* 1993; 27: 567 (erratum); *Int. J. Quantum Chem.* 1994; 51: 53.

Chemical Mechanism Reduction

*J. Garay, G. Li, N.J. Brown, and M.L. Koszykowski**

The control and reduction of air pollutants from combustion processes are important in maintaining air quality. Pollutants are minor species in combustion and the comprehensive kinetic mechanisms describing their formation and destruction are complex and frequently involve hundreds of elemental chemical reactions and tens of species. In most combustion systems, the species are not in equilibrium, and the success of a model with regard to the prediction of minor species depends on the accuracy of the representation of the chemical kinetics. Although we can model one-dimensional laminar flames for simple fuels with comprehensive chemistry, treating more complex flow fields with the same level of chemical detail is computationally demanding even with parallel computing. To simplify the chemistry, we have used advanced techniques of sensitivity analysis, namely, principal component analysis, to derive reduced mechanisms in H_2/air and CH_4/air systems.

Principal component analysis is an eigenvalue-eigenvector analysis of the matrix $\mathbf{S}^T\mathbf{S}$ where $\mathbf{S}$ is the sensitivity matrix of the normalized sensitivity coefficients and $\mathbf{S}^T$ is the transpose (Vajda and Turanyi, 1986). Sensitivities for the dependent variables (dimension $\mathbf{q}$) with respect to all input parameters (dimension $\mathbf{n}$) are computed at a number of grid points (dimension $\mathbf{m}$) to form the $(\mathbf{m} \times \mathbf{q}) \times \mathbf{n}$ matrix $\mathbf{S}$. The eigenvalues measure the significance of the eigenvectors in the overall mechanism. The eigenvectors represent sets of coupled reactions whose relative contributions are recognized by the relative size of the eigenvector elements. By defining a cut-off eigenvalue, a

*Sandia National Laboratories, Livermore, CA.

set of corresponding eigenvectors is found that divides the parameter space (reaction space) into a variant (influential) portion and an invariant (noninfluential) portion. The mechanism is reduced by including only those reactions that comprise the principal components (important eigenvectors). The eigenvectors carry information about connections among reactions that can be used to evaluate approximations like the quasi-steady state approximation. A hierarchy can be imposed by considering different values of cut-off eigenvalues; however, they are usually selected to maintain the precision of the model with respect to the variables of interest. The number of species is only reduced if elimination of reactions results in the exclusion of species.

Calculations of plug flow reactor (PFR), perfectly stirred reactor (PSR), and one-dimensional premixed laminar flame were carried out to reduce two hydrogen-air and two methane-air combustion mechanisms. One of the two H_2/air mechanisms was taken from the GRI methane/air mechanism[2]. The other was a new mechanism from the combination of the GRI mechanism and newly evaluated chemical kinetic data in the literature for H_2/air combustion. Zeldovich nitrogen chemistry was also included. The two methane-air mechanisms investigated were the Miller-Bowman 1989 mechanism and the GRI mechanism. The variables examined were major species, important radicals, NO, and temperature. Errors in all reduced mechanisms were required to be within 5% compared with the calculations using the comprehensive (unreduced) mechanisms.

The new and GRI mechanisms (each consisting of 28 and 34 reactions and 12 species) for hydrogen-air reduce to mechanisms that involve the same elementary steps. Hydrogen-air results showed that for the new H_2/air mechanism, a reduced mechanism with 23 reaction and 11 species was obtained that models all PFR and flame conditions considered. The rich PFR can be modeled with as few as 19 reactions and the lean with 20 reactions. Flames can be modeled with fewer reactions than PFR. An H_2/air mechanism consisting of 14 reactions and 11 species yielded NO profiles of precision equal to those generated from the full mechanism. Similar results were obtained for the GRI H_2/air mechanism. The methane-air results showed that the full Miller-Bowman (235 reactions and 51 species) and GRI (177 reactions and 31 species) mechanisms can be reduced to different mechanisms for different equivalent ratios. In the PFR calculations, for example, the comprehensive Miller-Bowman mechanism is reduced to 134 reactions and 38 species at =1 (Figure). PFRs require more reactions than flames because they are closer to strong ignition conditions. Rich methane combustion requires more reactions and species to model key radical species (CH, in particular). The rich methane flame can be modeled with 144 reactions. For the GRI mechanism, the mechanism reduction was controlled by being able to reproduce the CH profile over a range of equivalence ratios. A set of 125 reactions was found to be satisfactory for lean and stoichiometric mixtures, and 139 reactions were required for rich mixtures. The number of species associated with the reduced CH_4 mechanisms was in the range 30 to 40. The Miller-Bowman mechanism contains additional species that are not important in predicting our key major and minor species. The reduced mechanisms are weakly dependent on stoichiometry.

We have determined reduced mechanisms that can model a number of species profiles in flames, perfectly stirred reactors, and plug flow reactors over a range of input parameters including initial temperature, equivalence ratio, and

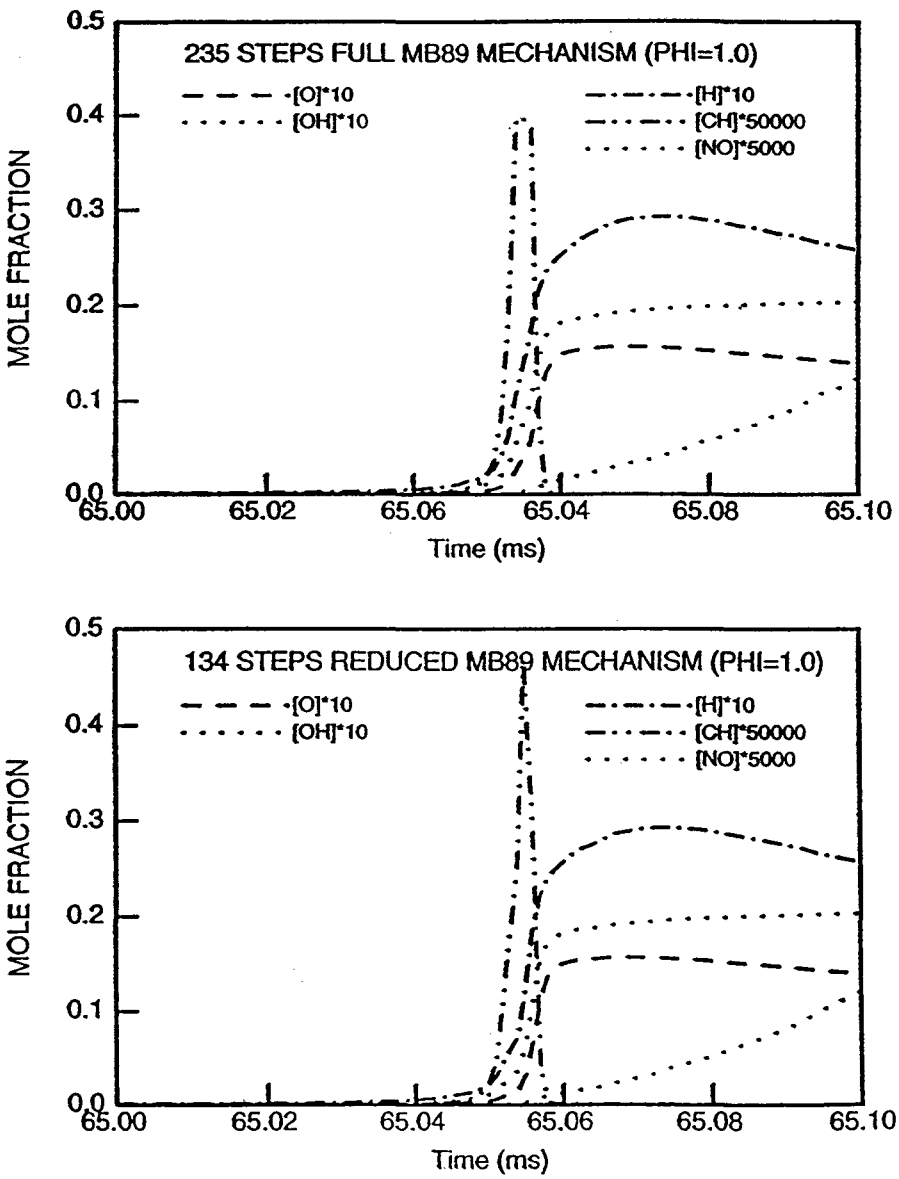

Figure. Comparison of species profiles in a PFR for the comprehensive and reduced Miller-Bowman mechanisms at PH1=1.

residence time for H_2/air and CH_4/air systems. We have also developed mechanisms that are suitable for generating temperature profiles. Principal component analysis was shown to be a reliable technique for the systematic reduction of complex chemical kinetics in combustion (Garay, Li, and Broom, 1994).

References

Vajda S, Turanyi T. *J. Phys. Chem.* 1986; 90: 1664-1670.

Frenklack M, Wang H, Bowman CT, Hanson RK, Smith GP, Golden DM, Gardiner WC, Lissianski V. "An Optimized Kinetics Model for Natural Gas Combustion." Abstract and poster, the 25th Symposium (International) on Combustion, Irvine, CA, 1994.

Garay J, Li G, Brown NJ. "Mechanism Reduction via Principal Component Analysis." Abstract and poster, the 25th Symposium (International) on Combustion, Irvine, CA, 1994.

Numerical Simulation of Combustion with Applications

G. Li and N.J. Brown

Some of the most important environment issues such as air pollution control and fire safety are directly related to very complex combustion phenomena that depend on the interactive processes between chemical kinetics and fluid mechanics. It is critical to understand the fundamentals of these coupled processes to predict combustion behavior. Although many simple or idealized combustion problems have been solved, a number of practical problems remain that are too complicated to be modeled exactly. Approximate models of these complex problems are computationally tractable and useful for providing insight into combustion behavior.

In order to reduce air pollution we have been investigating combustion characteristics of home gas appliances. Specifically, we have investigated combustion of a gas burner, which we approximated as a methane Bunsen burner. We have been using numerical modeling to investigate pollution production from Bunsen burner-type flames. The flames are actually two stage flames. The first state is a rich premixed flame, and the second, a burnout region, is a diffusion flame. The full investigation of a steady Bunsen burner flame involves a two-dimensional reacting flow calculation with detailed chemical kinetics describing methane combustion. Numerical solution of the problem is time-consuming even on a modern super computer; however, the problem can be simplified with a reduced mechanism and a boundary layer assumption. In order to estimate NO formation, the second stage burning of a methane-air Bunsen burner flame was modeled numerically using a two-dimensional boundary layer approximation.

In our simplified model of a Bunsen flame, the inner jet is of uniform composition and is characteristic of the products of a premixed flame of a specified equivalence ratio. The inner jet was surrounded by a co-axial jet of air. The flow rates of two jets are taken from Bunsen burner experiments from Nguyen *et al.* (1994). The initial temperature and species concentrations of the inner jet are determined from the solution of a one-dimensional burner-stabilized flame. A methane/air combustion mechanism of 185 reactions and 39 species was used in this model and was reduced from Miller and Bowman (1989; 1991) comprehensive mechanisms. The axial diffusions of momentum, energy, and species in this model are ignored because of the boundary layer assumption in the second stage diffusion flame model. The governing equations are thus assumed to be parabolic in the axial direction and are solved by marching down the axial direction. The boundary-layer equations of energy, momentum, and species are recast with the Von Mises transformation in which the cross-stream coordinate is replaced by the stream function as an independent variable. The equation of the stream function acts as a constraint on the momentum equation. A FORTRAN program, CRESLAF[1], was modified to solve the present problem of two reacting mixing jets surrounded by air at a constant pressure of 1 atm.

Equivalence ratios associated with the products of the first stage of the methane-air flame were in a range from 1.2 to 1.65. Two diffusion flames corresponding to the burning of the two fuels, H_2 and CO were identified in the second stage. There is enough difference in the diffusion velocities of the two fuels that their flames are separated by approximately 0.5 cm in axial distance. For a fixed axial location, the radial position corresponding to the maximum temperature and maximum product concentration was used to locate the diffusion flames. As illustrated in Figure 1, as

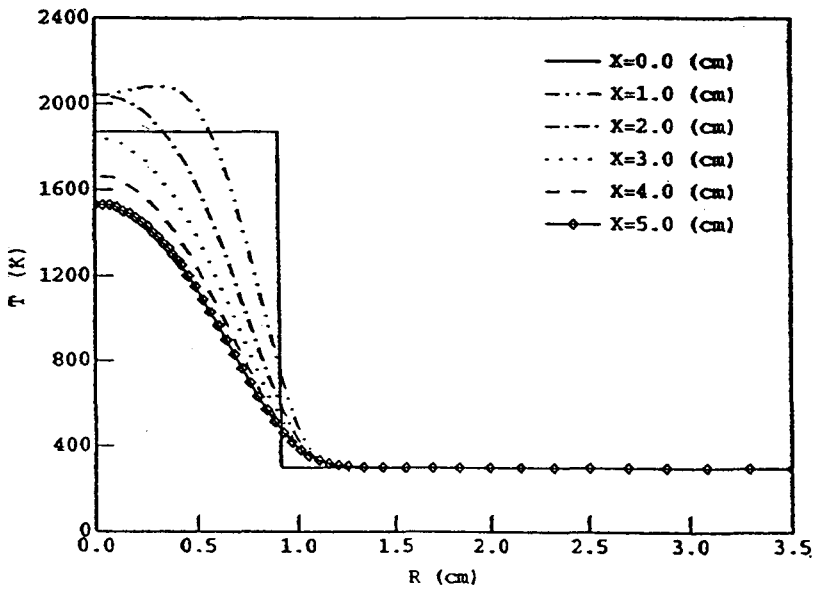

Figure 1. *Radial temperature profiles at different fixed axial locations for CH4 second stage burning for an inner jet initial composition and temperature characteristic of a burned flame of equivalent ratio 1.55.*

the fluid moves down stream, the location of maximum temperature moves toward the centerline of the inner jet, and the value decreases. NO production is dominated in the first-stage flame by the prompt NO mechanism and in the second stage by the thermal mechanism. The radial NO mole fraction profiles at different axial lodations are shown in Figure 2. Peak NO concentration locations are strongly influenced by temperature and O-atom profiles, and they are shifted to the right of the temperature maximum in the direction of the O atom maximum. Burnout of CO occurs rapidly at the location of the second diffusion flame. Second stage characteristics were not strongly dependent on first stage equivalence ratios. After scaling spatial coordinates to account for model approximations, computed profiles of OH, CO, and NO agreed satisfactorily with the measured values of Nguyen et al.

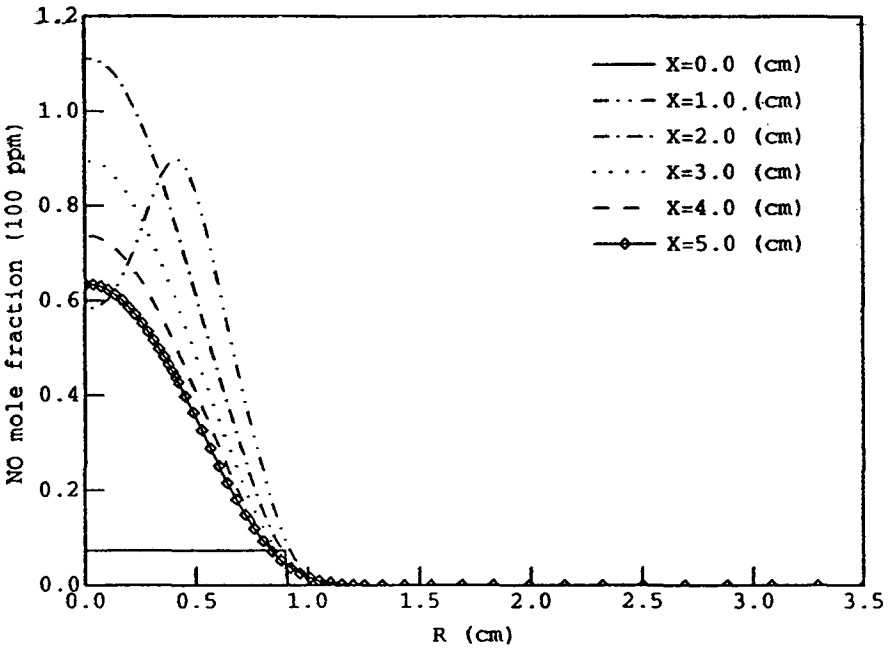

Figure 2. *Radial NO mole fraction profiles at different fixed axial locations for CH_4 second-stage burning for an inner jet initial composition and temperature characteristic of a burned flame of equivalent ratio 1.55.*

References

Coltrin ME, Moffat HK, Kee RJ, Rupley FM. *CRESLAF: A FORTRAN Program For Modeling Laminar, Chemically Reacting, Boundary-Layer Flow in Cylindrical or Planar Channels.* Sandia Report No. 93-0478, 1993. Sandia National Laboratory, Livermore, CA.

Miller JA, Bowman CT. *Prog. Energy Comb. Sci.* 1989; 15: 287.

Miller, J. A. and Bowman, C. T., 1991, Int. J. Chem. Kinetics, **23**, 289.

Nguyen QV, Edgar BL, Dibble RW, Gulati A. "An Experimental and Numerical Comparison of Extractive and In-Situ Laser Measurements on Nonequilibrium Carbon Monoxide in Lean-Premixed Natural Gas Combustion." 25th International Symposium on Combustion, the Combustion Institute, 1994.

Atmospheric Processes

Water Vapor Nucleation on Carbon Black and Diesel Soot Particles

G. Lammel and T. Novakov*

Aerosol nucleation properties, i.e. their ability to act as nuclei for cloud droplet formation (cloud condensation nuclei - CCN) at atmospheric supersaturation levels, are determined by the particle size, chemical composition, and surface characteristics. The CCN properties of water-soluble aerosols, such as sulfates, are well known. Much less is known about water vapor nucleation on carbonaceous (organic and black carbon) particles. Our experiments performed on El Yunque, Puerto Rico, and at Point Reyes, California, demonstrated that carbonaceous (organic) aerosols are a main contributor to CCN number concentrations at these sites. The apparent ability of organic aerosols to serve as CCN can have two possible explanations. The first is that the organic aerosols are inherently inactive and that condensation of H_2SO_4 vapor, or some other water-soluble species, onto these particles renders them active CCN. The second explanation is that a fraction of the chemically complex organic aerosol material is hygrophilic. In this study we attempt to relate the nucleation properties of carbonaceous particles to their water-soluble mass fraction.

In our experiments we used two kinds of carbonaceous materials, commercial carbon blacks and soot particles from diesel fuel combustion. To study the effects of altering the chemical characteristics of the carbon black aerosol, the initial materials were treated by digestion in diluted sulfuric acid, nitric acid, and bicarbonate. To change the

*Max-Planck-Institute for Meteorology, Karlsruhe, Germany.

sulfur content of the particles from the diffusion flame, thiophene was added to the diesel fuel. Adding thiophene increased the fuel sulfur content from the original ~0.5% to 4.4% (by weight). Chemical analyses of the aerosols and the carbon black starting materials for anions and cations were performed by ion chromatography. The water-soluble mass fractions of the materials were determined after ultrasonic treatment of the filter or impactor samples in deionized water.

Carbon black aerosols were generated in two ways–by resuspension of the dry materials and by atomization of aqueous suspensions. Combustion aerosols were produced by two sources using the same diesel fuel–an "alcohol lamp" in which the fuel is burned as a diffusion flame–and an idling bus engine (V8, mechanical injection). The polydisperse aerosol (a combination of resuspended dry carbon blacks and the combustion aerosol) was first passed through a one-stage impactor of 0.26-μm diameter cut-size and a bipolar charger (2 mCi ^{85}Kr) and then fed to a differential mobility analyzer (DMA). A stream of monodisperse, electrically neutralized particles was obtained by selecting the setting of the DMA electrode voltage and by passing the aerosol through a second bipolar charger (1.5 mCi ^{85}Kr). The number concentrations of the aerosol from the DMA were measured with a condensation nuclei (CN) counter. The number concentrations of particles activated to grow to droplets (CCN) were measured with a CCN counter as a function of both dry particle radius and supersaturation in the range from 0.2 to 1.3%.

From these measurements we derived an "activation radius," defined as the dry particle radius, for which 50% of all particles are activated at a fixed supersaturation, N(CN)/N(CCN) = 0.50. The nucleation ability of chemically modified carbonaceous particles increased with increasing soluble mass fraction and was comparable to that of $(NH_4)_2SO_4$ when the soluble mass fraction exceeded about 10%. The hygroscopicity of particles generated by combustion of diesel fuel in a diffusion flame increased when a sulfur-containing compound was added to the fuel. The CCN characteristics of diesel soot appear to be comparable to that of wood smoke aerosol, known to be CCN active.

Organic Aerosols and Cloud Condensation Nuclei at Point Reyes, California

C.A. Rivera-Carpio, C.E. Corrigan, J.E. Penner, and T. Novakov*

Anthropogenic aerosols may affect climate directly by scattering and absorption of solar radiation and indirectly by influencing the number concentration of cloud droplets (and the albedos of clouds) through their ability to act as cloud condensation nuclei (CCN). In contrast to direct aerosol effects, quantitative assessment of indirect aerosol effects is more difficult because of its greater complexity and the many open questions that remain to be answered. One of these questions pertains to the chemical identity of CCN. So far sulfate aerosols have received the most attention in assessing both the direct and indirect aerosol effects on climate because of their relatively well-documented global distribution and known optical and nucleation properties. In view of the fact that sulfate species are not the only component, and sometimes not even the dominant component, of submicron aerosol mass, it can be expected that aerosol constituents other than sulfate will contribute to the CCN concentrations, at least in some environments. Indeed, comparisons of CCN number and sulfate mass concentrations in the Caribbean and elsewhere have suggested that a substantial fraction of measured CCN concentrations cannot be explained by sulfate aerosol alone. An analysis of our data obtained on El Yunque peak, Puerto Rico, has shown that these non-sulfate CCN are most likely derived from organic aerosols.

A prerequisite for assessing the potential role of non-sulfate CCN is the development and validation of methodologies for apportioning the contribution of mass concentrations of major aerosol species to total CCN concentrations. In this report we outline our approach to this task. Our experimental strategy is based on the assertion that the CCN concentrations can be calculated from the dry aerosol number size distribution if the relationship between the dry size and supersaturation of aerosol particles is known. Therefore, if one could express the number size distribution as a sum of contributions of the mass concentrations of major aerosol species to the total number size distributions, then the contribution of these species to the CCN number concentrations could be determined, assuming that a relationship between particle size and supersaturation can be empirically defined.

Our approach involves concurrent measurements of mass size distributions of inorganic and organic aerosol components, aerosol number size distributions, and CCN concentrations (measured at 0.5% supersaturation) in October, 1993, and June/July, 1994, at Point Reyes, California. The data analysis consists of converting mass size distributions to number size distributions, comparing the derived and measured number size distributions, determining the number concentrations of particles in size ranges that correspond to the measured CCN concentrations, and estimating the contributions of major aerosol chemical species (sulfate, organic, and seasalt) to the CCN number concentrations.

Aerosol particles were sampled by the micro-orifice uniform deposit impactor (MOUDI). Mass size distributions of major aerosol species were obtained by applying a data inversion method to the raw MOUDI data. Mass size distributions of individual aerosol species were converted to cumulative number size distributions of total aerosol and individual components. From these the contributions of major aerosol components (such as sulfate, organic and seasalt) to CCN concentrations at a fixed supersaturation were estimated.

Our results demonstrate that the contributions of mass concentrations of major aerosol species (sulfate, carbonaceous material, and NaCl, a substitute for seasalt) to CCN number concentrations can be reasonably accurately estimated from measured mass size distributions of these species. The derived and measured number size distributions were found to be in good agreement. Our results demonstrate that the contributions of organic

*Global Climate Research Division, Lawrence Livermore National Laboratory

and sulfate aerosols to CCN number concentrations at Point Reyes are variable and range from ~20 to ~65% for sulfate and ~5 to ~80% for organic aerosol. The principal factor influencing the SO_4^{2-} and organic mass contributions to CCN is the mass concentration of these species found in the sub-0.1 μm range, which dominates the aerosol number concentrations. Dependence of the derived total CCN concentrations on supersaturation shows that these decrease with supersaturation. However, when carbonaceous aerosols contribute significantly to the CCN concentrations at 0.5% supersaturation, their contribution remains significant, even at supersaturation values as low as 0.1%.

An obvious question is: How important are organic CCN in the broader climate picture? A recent modeling study of indirect aerosol climate forcing excluded non-sulfate (presumably organic) aerosols. The authors of this study argued that the neglect of these aerosols should not result in a large underestimate of the indirect radiative forcing because of the nonlinearity of the response of cloud droplet concentrations to increasing CCN concentrations, if it is assumed that the anthropogenic sulfate and non-sulfate emissions are similar in the affected areas. This assumption, however, may not always be valid: the emissions of SO_2, the precursor of anthropogenic sulfate aerosol, depend on the amount of fuel burned, its sulfur content, and the presence or absence of emission controls. Anthropogenic combustion-derived carbonaceous aerosols (primary and secondary organic and black carbon components) are products of incomplete combustion, only partly related to the amount of fuel and essentially unrelated to its sulfur content. A cursory examination of regional SO_2 and CO (an indicator of incomplete combustion) emissions illustrate this point. The CO (Mt/yr)/SO_2 (Mt/yr) emission ratios for the United States, in the states west and east of Mississippi River (in 1985-87), were 6.2 and 2.8, respectively, reflecting different fuel uses in the western and eastern United States. Clearly, the relative abundances of sulfate and carbonaceous aerosols over these regions are expected to be different. Indeed, an examination of ambient sulfate and organic aerosol mass concentrations measured at remote locations in the United States shows that organic aerosols dominate or are equal to sulfate in the western United States, while sulfate dominates over organic carbon in the eastern United States.

Analytical Expression for CCN Activation Spectra of Atmospheric Aerosols and Its Application to the Interpretation of CCN Concentration Data

C.A. Rivera-Carpio

An analytical expression for the number concentration of cloud condensation nuclei (CCN) as a function of supersaturation, i.e. CCN activation spectra, has been developed. (CCN are hygroscopic aerosol particles on which cloud droplets form.) The expression describes the dependence of CCN concentration on supersaturation in terms of CCN dry size distribution and activation parameters. It is based on parametric representations of both the size distribution and the dry size to critical supersaturation relationship. The size distribution is represented using three log-normal functions. The relationship between the dry size and critical supersaturation of hygroscopic aerosol particles is described using a power function in terms of activation parameter. The three log-normal description is consistent with observed total aerosol size distribution and the power-law type description is supported by observations. Both of these descriptions are general and warrant the successful application of the resulting analytical expression for the CCN activation spectra.

This analytical expression offers the possibility of interpreting CCN concentration data in terms of their activation and physical (size distribution) parameters. It allows estimation of these CCN parameters from CCN concentrations measured at several supersaturation ratios. Data on CCN activation are very limited whereas data on CCN size distribution is essentially non-existent. (CCN size distribution is assumed to be equal to the total aerosol size distribution above a given size.) If such information were available, then it would be possible to assess geographical and temporal variations in CCN concentrations and to identify the predominant factors responsible for such variations (CCN climatology). Furthermore, concurrent determination of the physical and activation characteristics of CCN provides the information needed to estimate the water-soluble and water-insoluble volume size distributions of CCN active particles. If CCN water-soluble and water-insoluble volume size distributions were available, then it would be possible to deduce (from chemical analysis of size-segregated aerosol samples) not only CCN constituents but also the CCN water-soluble constituents. Information on CCN composition is very much needed in order to assess the potential climate effect of sulfate aerosol through CCN-cloud albedo modulation. In contrast to aerosol sampling for chemical analysis, CCN sampling involves complicated and expensive instrumentation and sampling periods of several days.

A practical method to interpret CCN concentration data sets in terms of CCN activation and number size distribution characteristics has been developed. The method involves setting a system of analytical equations and solving it for the activation and hygroscopic size distribution parameters. The input data are CCN concentrations at a relatively small number of supersaturation ratios. The size of the data set is equal to one plus the number of modes of the aerosol size distribution. The method is based on the assumption that with each mode of the total aerosol size distribution there is an associated hygroscopic aerosol size distribution mode equal to an unknown constant fraction of the aerosol mode. The method allows testing of the more restrictive assumption usually made for the CCN size distribution, i.e., CCN size distribution equal to the total aerosol size distribution above a minimum size. There is increasing evidence that when CCN concentrations are high, this customary assumption does not apply. The evaluation of the method involves comparison of the estimated CCN activation and physical characteristics against measurements.

Parametrization of the Fraction of Activation of Atmospheric Aerosols

H. Abdul-Razzak, S.J. Ghan†, and C.A. Rivera-Carpio*

We have developed a parametrization scheme of the fraction of aerosol particles activated to form cloud droplets in a parcel of air rising adiabatically. The result applies to aerosols of a single log normal size distributed, water-soluble type (i.e., capable of serving as cloud condensation nuclei) with uniform chemical composition. The parametrization scheme is based on analysis of the rate equations for the parcel's supersaturation and the aerosol's nucleation process. The analysis led to identification of only four dimensionless parameters on which the fraction of activation strongly depends. Using results of detailed numerical simulations by a size-resolving Lagrangian parcel model, errors due to simplifying assumptions used in the analysis were largely eliminated by employing adjustment coefficients. For a wide range of governing parameters (e.g., particles' mode radius, size spread, updraft velocity, etc.), differences between the parametric equation's and the numerical model's results are less than 10%. For extreme yet realistic conditions, errors are less than 25%. This new parametrization is significantly more accurate and successful in representing the fraction of activation in terms of governing parameters than any known parametrization.

*Texas A&M University, Kingsville, TX
†Pacific Northwest Laboratory, Richland, WA

Ecological Systems

Heavy Metal Environmental Contaminants: Toxicology and Bioremediation

R.J. Mehlhorn, K. Brouwer, I. Fry, K. Moore and Y.-R. Wu

Heavy metals contaminate many areas of the world and threaten the health and safety of human communities and the integrity of ecosystems. Considerable effort is underway or is being planned for decontaminating polluted environments. While most environmental restoration efforts to date have focused on organic pollutants, increasing attention is being devoted to heavy metal decontamination. Unlike organic pollutants, which can be biodegraded to non-toxic products, metals can only be sequestered to decrease their bioavailability or, in a few cases, can be manipulated by chemical or biological means to induce valence transformations that decrease their toxicity or to combine with complexation agents to form non-hazardous products. Valence transformations of metals are normal geochemical processes associated with the movement of matter into or out of contact with atmospheric oxygen. Biological reductions and oxidations often play a rate-determining role in such geological processes but details of how these reactions function in the heterogeneous environments of the Earth's surface are not well understood. An improved understanding of biological interactions with heavy metals could create opportunities to manipulate biological systems to stimulate valence transformations and mineralization processes and to use such manipulations for environmental remediation.

Apart from remediating known contaminated environments, society must learn to manage more effectively the release of hazardous chemicals by both established and newly emerging industries. New industries may generate waste whose health hazards may become apparent only at some future time. Modifications of industrial processes, ideally culminating in "zero discharge" are therefore the preferred means of pollutant control. An understanding of heavy metal toxicity mechanisms, which is being sought in our research project, is important for designing industrial process modifications that are appropriate and cost-effective. Among the important toxicity mechanisms of heavy metals is their potential for promoting free radical processes. Our project on cigarette smoke toxicity has demonstrated that transition metal release from proteins catalyzes destructive free radical reactions. We have shown that hemoglobin damage by tobacco smoke oxidants releases iron, which catalyses free radical formation via so-called active oxygen species. The study of oxygen activation by free iron has given us valuable insights into some parallel mechanisms of action of hexavalent chromium, an important environmental carcinogen. We have discovered that pentavalent chromium is stabilized by a number of biological ligands to form a persistent catalyst of free radical production, which probably plays an important role in chromium toxicity.

Our third project is developing biological agents for the recovery of textile colorants from dye baths, thus setting the stage for modifying the dyeing process to avoid the release of colorants and chemicals into discharge waters and allowing for re-use of valuable resources. We have made considerable progress in producing biomass for removing widely-used textile dyes from dyebaths and have demonstrated the feasibility of recovering completely decolorized waters containing a variety of chemical additives that can be fed back into the process stream. Moreover, our data suggest that process modifications using the biomass

as a reversible dye sorbent will allow for the recovery of dyes for re-use, thus augmenting the economic benefits of recovering other dyebath components.

Purpose

We seek an understanding of how heavy metals and polycyclic aromatic hydrocarbons interact with biological systems and to exploit that understanding for technology development. Our studies comprise the elucidation of heavy metal toxicity mechanisms, which includes the development of sensitive damage markers, and the production of biomass-derived sorbents for removing and recovering heavy metals, toxic organic molecules or valuable chemicals from water and soil.

Methods

Our principal experimental approach is electron spin resonance (ESR), a highly specific method that detects the magnetic moments of reactive free radicals, transition metal ions and "spin-labeled" organic molecules. During the past year this method has been used to analyze biological structures with the goal of optimizing biomass applications for heavy metal removal and resource recovery in aqueous solutions. ESR has also been used to develop a sensitive chromium speciation method, which has enabled us to observe chromium metabolism in living suspensions of microbial cells. Finally, we have developed novel ESR markers of free radical damage; these are being developed in the human red blood cell (erythrocyte) and are being applied to the analysis of tobacco smoke toxicity.

Research Highlights

Chromate reduction by Baker's Yeast (Saccharomyces cerevisiae):

Saccharomyces cerevisiae, an organism that poses no health risk and can be produced inexpensively as well as stored in a dehydrated state for prolonged periods prior to use in aqueous cell suspensions, was shown to reduce carcinogenic hexavalent chromate to the less hazardous and less water-soluble trivalent chromium species (collaboration with Paula Krauter, LLNL). Disappearance of chromate as well as an appearance of pentavalent chromium, stabilized by complexation with sorbitol, in the extracellular phase of metabolically active cell suspensions, were demonstrated. A substantial fraction of the final reduction product of hexavalent chromium was trivalent chromium, which was detected in the extracellular bulk aqueous phase and which could readily be separated from the cells by centrifugation. This finding complements our previous report of chromate reduction by *Bacillus subtilis*, a soil organism that also reduces hexavalent chromium but that, unlike the yeast, unfortunately has been associated with some human health risks.

Antioxidant depletion is a toxicity mechanism of cigarette smoke

Our recent tobacco smoke experiments have improved the understanding of how inhalation of the smoke leads to cardiovascular disease, cancer and many other health problems. We have demonstrated that exposure of blood to either unfiltered and gas-phase cigarette smoke rapidly depletes cells of vitamin C and glutathione. Like vitamin C, glutathione can act as an antioxidant to protect against free radical damage. However, glutathione has many other important protective functions including its vital role in removing non-radical carcinogens. We have also obtained data demonstrating the damage-enhancing effects of oxidants by hydrogen cyanide, which has long been known to be present in cigarette smoke. Treatment of blood with cigarette smoke inhibits the enzymes catalase and superoxide dismutase. Loss of catalase function in cigarette-smoke-exposed blood is characterized by an accelerated oxidation of hemoglobin and glutathione by hydrogen peroxide.

References

Mehlhorn RJ, Buchanan BB, Leighton T. "Bacterial Chromate Reduction and Product Characterization." In: *Emerging Technology for Bioremediation of Metals* (J.L. Means and R.E. Hinchee, eds.). Boca Raton, FL: Lewis Publ. (CRC Press) 1994: 26-37.

Mehlhorn RJ. "Oxidants and antioxidants in aging." In: Phys*iological Basis of Aging and Geriatrics* (P. Timiras, ed.). Boca Raton, FL: CRC Publ., 1994: 63-75.

Fry IV, Mehlhorn RJ. "Polyurethane and Alginate Immobilized Algal Biomass for the Removal of Aqueous Toxic Metals." In: Emer*ging Technology for Bioremediation of Metals* (J.L. Means and R.E. Hinchee, eds.). Boca Raton, FL: Lewis Publ. (CRC Press) 1994: 130-134.

Predicting Chronic Toxicity in Aquatic and Terrestrial Ecosystems

S. Anderson, W. Sadinski, J. Hoffman, J. Jelinski, D. Steichen, G. Garman, M. Wilson, G. Wild and J. Harte

The broad goal of this project is to elucidate the chronic and sublethal effects of exposure to toxic substances on aquatic and terrestrial ecosystems. We have recently conducted research in two major areas. These are genetic ecotoxicology and sediment toxicity in San Francisco Bay.

Linking Genotoxic Responses and Alterations in Reproductive or Developmental Success

Relationships Between ^{32}P-Postlabelled DNA Adducts, Micronuclei, and Fitness Parameters in Xenopus laevis exposed to Benzo[a]pyrene

We studied effects of benzo[a]pyrene (B[a]P) on inductions of hepatic adducts and erythrocytic micronuclei in *Xenopus laevis*. We also examined associations of such inductions with wet weight and development immediately following exposure and at metamorphosis. In the ecological literature, time to metamorphosis has been related to fitness due to the necessity for larvae to attain metamorphosis before larval habitats become dry. Size at metamorphosis can be associated positively with reproductive success. Erythrocytic micronuclei have been shown to be reliable measures of sublethal DNA damage in some amphibians, but ^{32}P-postlabelled DNA adducts have not been reported previously. In addition, relationships between biomarkers and sublethal effects on fitness remain poorly understood in any species.

Increased DNA adducts, micronuclei, and time to metamorphosis were all positively associated with exposure to B[a]P (Fig.1). DNA adducts and micronuclei increased as a function of exposure to 31 and 248 nM B[a]P for 14 days (Sadinsky et al., in press) and exposure to 248 nM for 2, 4, 8, and 16 days. Sensitivities and frequencies of micronuclei and adducts were similar for both measures. Frequencies

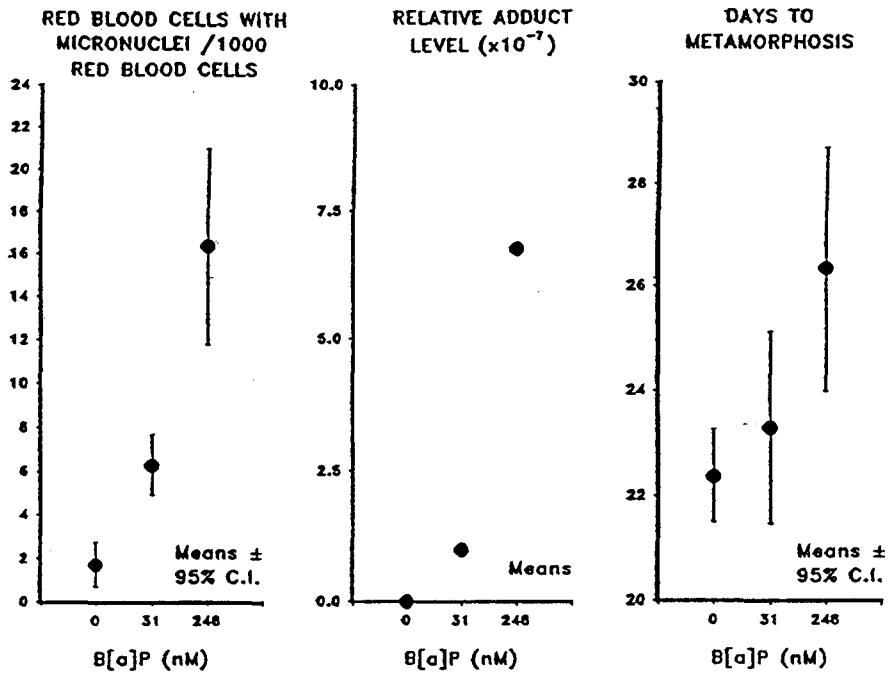

Figure 1. *Sterile frequency in C. elegans following multigeneration exposure to EMS.*

were associated positively with time to metamorphosis at 248 nM, but there was no effect on time to metamorphosis at 31 nM, or wet weight at metamorphosis at any dose. Frequencies were associated negatively with wet weight and developmental stage at 16 days, but only with wet weight at 14 days.

It appears that DNA adducts and micronuclei can be both sensitive measures of sublethal DNA damage and short-term indicators of effects on fitness in amphibians. Research with native species and wild populations is necessary to determine whether these markers can be useful in studies of declining amphibians. Further studies of associations between biomarkers of effective dose and sublethal effects on fitness are needed. This project was conducted in collaboration with Dr. Bill Bodell at UCSF. To our knowledge, this research has provided the first example of a correlation between sublethal genotoxic responses and established fitness parameters.

Multigeneration responses following exposure to genotoxic agents in the nematode Caenorhabditis elegans

We assessed brood size and sterility in multigeneration exposures of the nematode *C. elegans* to ultraviolet-B (UV-B) and ethyl methane sulfonate (EMS). In the UV-B experiments, an initial 50% decline in broodsize of UV-B exposed worms was noted and maintained in every subsequent generation (Fig. 2). In contrast, the occurrence of sterile progeny followed an unusual pattern of multigeneration effect. For six generations, there were no sterile progeny. Following the sixth generation, there was a steep linear increase in sterile progeny. At 15 generations, the experiment was terminated because nine of the original 12 replicates no longer produced viable progeny. In contrast, all of the 12 control replicates produced viable progeny for 15 generations.

Progeny of animals exposed to EMS for one and two generations had mean frequencies of steriles of 0.0 and 0.8×10^{-2}, respectively. In contrast, progeny of animals exposed for three and four generations produced frequencies of steriles of 14.8×10^{-2} and 25.8×10^{-2}. In four successive generations, progeny of control animals elicited sterile frequencies of 0.0, 1.6, 0.8, and 1.6×10^{-2}.

These data indicate that multigeneration effects on the frequency of sterility, and in some cases broodsize, are clearly discernable. However, we have not determined the mechanism of multigeneration change. We attempted to determine whether mutation frequencies increased at each generation of exposure; however EMS caused minor developmental asynchrony in the cultures that introduced bias into the mutagenesis assay. The data did indicate a potential increase in mutation frequencies among generations, but they are viewed only as suggestive. This research was conducted in collaboration with Dr. David Littlejohn of the Flue Gas Chemistry Group.

Induction of DNA-protein crosslinks in developing embryos of the purple sea urchin Strongylocentrotus purpuratus

Exposure to genotoxic agents such as certain chemicals and UV light during embryonic development may result in DNA-protein crosslinking (DPC). DPC has been demonstrated for mammalian cell lines (Zhitkovich and Costa, 1992), and formation of DPCs upon exposure to a wide variety of agents including some metals has been observed. To determine whether DPCs could be detected in sea urchin embryos during development, we adapted a mammalian cell assay utilizing potassium-SDS precipitation and a DNA

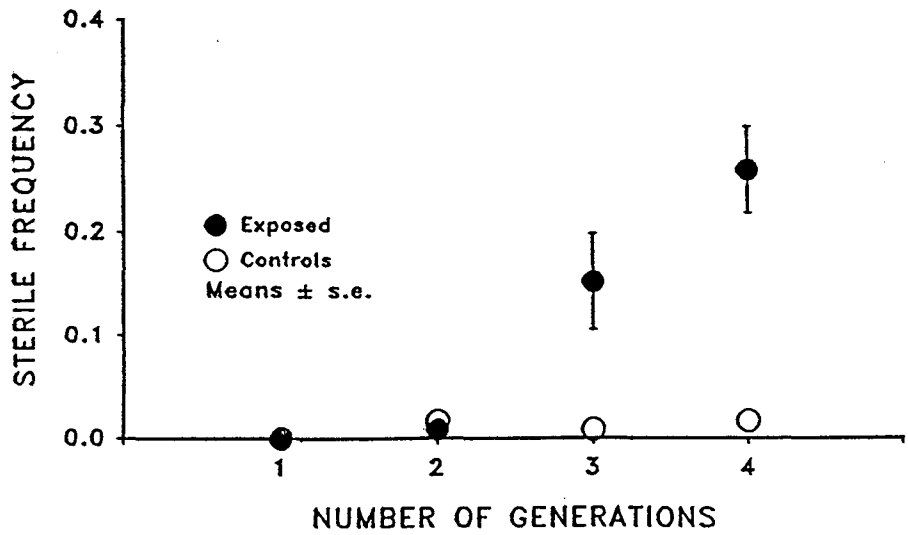

Figure 2. *Effects of B[a]P exposure on larval Xenopus laevis.*

fluorochrome to quantify relative amounts of free and protein-bound DNA.

Sea urchin embryos exposed to a known DPC agent, nickel (Ni, 0.5-6 mM) through gastrulation exhibited a dose-dependent increase in DPCs, as well as an increase in developmental abnormalities. Similar results have been observed with chromium, and studies with arsenic are underway. Morphological studies demonstrated that stage-specific exposure to Ni prior to gastrulation resulted in similar levels of abnormal pluteus larval development as compared to embryos exposed continuously through gastrulation. Sea urchin embryos exhibit temporal differences in DNA transcription and gene expression during development, and these could be affected by modification in DNA-protein interactions. Therefore, we are also investigating the hypothesis that similarities in morphological responses we observed may relate to susceptibility of a critical stage of development (e.g., pregastrula) to DPC.

This research is being conducted in collaboration with Dr. Gary Cherr at the the University of California Bodega Marine Laboratory. It has provided an important new technique for molecular dosimetry of exposure to selected metals and indicated strong associations between a measure of biologic dosimetry and altered developmental success. We will build upon these findings in studies on arsenic and nickel at mining sites.

Arsenic effects in model animals

We have evaluated the effects of arsenic exposure on the induction of micronuclei in *X. laevis* tadpoles, mutagenesis in *C. elegans*, and dominant lethal mutations (hatching rate) in *O. latipes*. Tadpoles were exposed for 14 days to 5 sublethal concentrations (0, .1, 1, 5, 10 and 15 mg/l) of arsenate (As V). Blood was extracted by microcapillary pipet. No significant increases in micronuclei were noted. In addition, a significant dose-dependent *increase* in wet weight was observed. Because 20 mg/l is lethal to the tadpoles, we were confident that the doses were properly selected. However, we do not know whether micronuclei would be observed if additional sampling times were used in the experiment. A weak positive response was observed in the nematode mutagenesis assay, but only at a high dose of 50 mg/l arsenate (AsV). Thus mutagenic effects of AsV occurred at much higher doses than those that induced reproductive impairment in the pore water assay. This may be due in part to the fact that a four-day exposure was conducted for the reproduction assay; whereas, a one-day exposure was the maximum time used for mutagenesis. Work with the medaka dominant lethal assay is still underway. However, preliminary data indicate that predominant effects of AsV exposure are on egg production not hatching (dominant lethal mutations) and that effects are observable only at the relatively high dose of 12.5 mg/l.

Genotoxic effects of arsenic exposure may not occur at levels lower than those that affect development. Embryonic abnormalities in a variety of species including amphibia and sea urchins are induced at approximately 100-200 µg/l. Consequently, ecosystem studies should concentrate on direct comparisons of development and genotoxic effects on early lifestages wherever possible. Our primary goal in the next year is to develop a cytogenetic assay utilizing tadpole limb buds and/or embryos of *X. laevis*, or a native species of amphibian.

Napa Conference on Genetic and Molecular Ecotoxicology

This conference was a major effort for our laboratory in the last year. Under the auspices of Dr. Anderson's Pew Scholarship in Conservation and the Environment, she conceived of a conference to unite the thinking of genetic ecotoxicologists with ecological and population geneticists. The concept for the conference received recognition and was eventually funded by NIEHS. The organizing committee included Dr. Anderson, Dr. William Suk (NIEHS Superfund Program Project Director), and Dr. Lee Shugart (Oak Ridge National Laboratory). Forty scientists from around the world were invited to attend and to contribute their thoughts toward a framework for future research in the field. The major product of the conference is a peer-reviewed issue of *Environmental Health Perspectives (Supplement)* which was edited by Dr. Anderson. Twenty-one papers have been published in the issue (available December, 1994), and one will describe the research framework discussed above (Anderson et al., 1994). The paper summarizing Dr. Anderson's presentation at the conference is also included in the conference proceedings (Anderson and Wild, 1994). Judging from follow-up letters from numerous participants, the conference was viewed as a watershed event in the field.

Sediment Toxicity in San Francisco Bay

Our goal was to determine whether pore water toxicity tests can be used to develop site-specific sediment quality objectives as well as to reliably characterize differences in toxicity among sites. Pore water was prepared by centrifugation of sediment grab samples, and toxicity tests included echinoderm 48-hour embryo development, bivalve embryo development, and amphipod survival. Dose responses were observed using spiked pore water bioassays with nickel for all three species. EC50 values for nickel did not vary significantly among sampling periods at a single reference site. Sediment to pore water distribution coefficients were determined to enable prediction of the bulk sediment concentrations of nickel that may cause detrimental effects. Intrasite variability was characterized in repeated studies at one reference site. Intrasite variability is comparatively low for all tests. For example, field replicate mean values (± std error) for abnormal development in *Mytilus edulis* embryo tests ranged from 79.7 ± 1.7% to 86.6 ± 1.7% for three sampling periods. A range of toxic sites within the Bay are clearly discernable from the reference station. We conclude that pore water toxicity tests will be useful in various applications for sediment quality management in San Francisco Bay. This research was conducted in collaboration with Dr. John Knezovich of the Lawrence Livermore National Laboratory.

References

Anderson S.L., Hose J., Knezovich J. Genotoxic and developmental effects in sea urchins are sensitive indicators of effects of genotoxic chemicals. *Environmental Toxicology and Chemistry*. 1994; 13(7).

Anderson S.L. "Global Ecotoxicology: Management and Science." In: R. Socolow, C. Andrews, F. Berkhout, V. Thomas, eds. *Industrial Ecology*. Cambridge University Press, 1994.

Anderson S., Wild G. Linking genotoxic responses and reproductive effects in ecotoxicology. *Environmental Health Perspectives*, Vol. 102 Supplement 12:3-8, 1994.

Anderson S., Shugart L., Sadinski W., Brussard P, DePledge M, Ford T, Hose J, Stegeman J, Suk W, Wirgin I, Wogan G. Genetic and molecular ecotoxicology: a research framework. *Environmental Health Perspectives*, vol 102 Supplement 12:9-12, 1994

Sadinski W, Wilson M, Hoffman J, Levay G, Bodell W, Anderson S. Relationships among ^{32}P-postlabelled DNA adducts, micronuclei, and fitness parameters in *Xenopus laevis* exposed to benzo[a]pyrene. *Aquatic Toxicology* (in press).

Predicting Optical Properties of Marine Aerosols

M.S. Quinby-Hunt and A.J. Hunt

This project studies the scattering properties of aerosols in the marine boundary layer (MBL) and their effects on visibility, light propagation, radiant transfer, and global albedo. We determine what polarization parameters are the most useful to characterize and how to classify the dominant components of MBL aerosols. The project will explore the merits of using polarized light scattering to study the formation of, and variability in, aerosols in the MBL. The predicted variability of polarized light scattering due to the various components of aerosols in the MBL is modelled to establish the need and viability of measuring polarized light scattering *in situ*.

Particles in the MBL affect visibility, cloud formation, radiative transfer, and the heating and cooling of the Earth. Dense MBL hazes modify the propagation of sunlight effecting both the intensity and polarization of light reaching the sea surface. Both these quantities must be included in radiant transfer calculations at the surface of and within the ocean. Aerosols in the MBL affect visibility because the scattered light reduces the contrast between the viewed scene and the background. Near-forward scattered light is most effective in reducing contrast of a naturally-lighted scene and thus is dominated by the large particles in the aerosol. If the scene is illuminated by a source near the detector, backscattered light is most important in reducing contrast. Conversely, sunlight or moonlight scattered into the detector from along the target-detector path also reduces contrast. Since scattering can occur at any angle, it can be caused by particles of nearly any size. Thus, depending on the situation, aerosol particles of all sizes are important in determining visibility.

The angular dependence of the linear and circular polarization of light scattered by aerosols in the MBL provides the most complete information regarding the aerosol characteristics obtainable by remote sensing. Measurements of the polarization properties of aerosols can be used to infer effective size distributions and refractive index of marine aerosols without the problems of collection devices. The limited research on the scattering properties of atmospheric aerosols has been primarily with terrestrial aerosols. Few studies have investigated the polarization properties of scattered light in marine aerosols and even fewer using the fullest description of the polarization as embodied by the Mueller scattering matrix formalism.

Mie scattering models are being used to calculate the polarization properties of light scattered from combinations of Junge, Gaussian, and skewed distributions of spheres and coated spheres of varying composition and refractive index. These models are used to calculate the scattering from observed distributions of particles in the MBL representing a variety of marine environmental conditions. Models are verified by comparison of scattering measured in the laboratory with that predicted by calculations.

Model Verification

The results of the models were verified by comparison to scattering from $(NH_4)_2SO_4$ particles, a component of aerosols in the MBL that is nearly spherical and readily generated in the laboratory. At both 325 and 633 nm, the LBL model agreed with both the $(NH_4)_2SO_4$ data and earlier calculations.

To determine whether the scattering predicted by a commonly used model of the aerosols in the MBL (Shettle-Fenn, *Models for the Aerosols of the Lower Atmosphere and the Effects of Humidity Variations on Their Optical Properties*, 1979) deviates from the Rayleigh approximation and varies with humidity, scattering predicted for a typical marine aerosol was calculated at 50%, 80% and 99% RH. Varying the humidity has a small impact on the polarization properties at angles > 150°. The total intensity of scattered light increases with size indicating that the size effect is greater than the decreasing polarizability caused by the increased RH which dilutes the concentration of solute in the particles lowering index of refraction. If the relative number of sea salt particles is increased (as might occur under increased wind and wave action), scattered light polarization deviates further from the Rayleigh approximation. As the sea salt component increases the linear polarization changes from positive to negative at roughly 150°, indicating a change from horizontal to vertical polarization.

Measurements of number distributions of particles in the MBL show a component larger than the Rayleigh-like component ($r_{mode} \sim 0.03\,\mu m$) and smaller than the sea salt (maritime) component of Shettle and Fenn. The exact r_{mode} and relative contributions of each of these components varies with RH, wind speed and distance from land. For the purpose of comparison to the Shettle-Fenn model, we calculated the scattering of an aerosol composed of two components which represent the average of observations typical of conditions with no continental influence plus a marine, primarily sea salt, component as described by Shettle and Fenn. The scattering predicted using experimental (Hoppel *et al.*) components differs significantly from that of the Shettle-Fenn model (Figure 1). The degree of linear polarization (S_{12}) decreases significantly at 90° and that the peak polarization is shifted to higher angle. The absolute value of S_{34} is much larger.

Effect of Soot on Scattering in the MBL

To explore the presence of a widely occurring and highly absorptive component in the MBL, scattering from carbon soot was calculated. In coastal areas and near shipping lanes soot can be an important component of marine aerosols. This component may affect on scattering significantly, because the real and imaginary parts of the refractive index are large. To further complicate matters, the reported refractive index varies considerably—from $n = 1.4\text{-}0.13i$ to $2.29\text{-}0.87i$—which may indicate real variation among soots depending on source. This is probably due to incomplete combustion, non-fully dense agglomerations of carbon particles, or the presence of homogeneous low- to non-absorptive products in the aerosol. Size distributions also vary considerably. Soots derived from the oil fires in Kuwait collected at 1-6 km altitude (considerably above the MBL, but of practical interest as they were collected in the field) showed a broad distribution of particle sizes. These were approximated as a broad log normal distribution adjusted to roughly fit the number distribution reported at 3.7 km altitude and 160 km from Kuwait. For this broad distribution of sizes, the linear polarization is dramatically reduced. S_{34} actually changes sign at angles > 60°. As agglomerated particles are not necessarily spherical, the scattering should be calculated using approximations that can account for deviations from sphericity.

Conclusions

The polarized scattering predicted for the MBL is not Rayleigh-like. Scattering is sensitive to the details of the size

and number distributions and therefore may be used to discriminate various aerosols. Knowledge of the predominate character may be used to choose polarimetric sensing methods that discriminate against scattered ambient light in the MBL. The effects of the size, number density, real and imaginary indices of refraction and particle shape all have significant effects on the polarization characteristics of the scattered light and potentially on visibility.

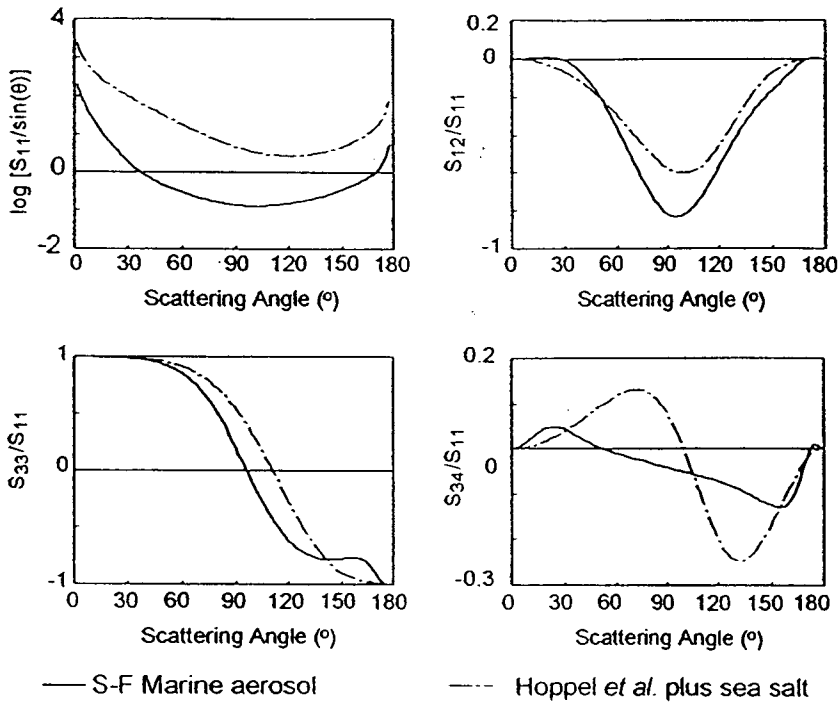

Figure. *Comparison of the Shettle-Fenn marine aerosol with an aerosol made up of the ~0.02 μm and ~0.1μm components observed by Hoppel et al. plus a sea salt component.*

References

Quinby-Hunt MS, Hull PG, Hunt AJ . Predicting polarization properties of marine aerosols. *Proc. SPIE, Ocean Optics XII*, 13-15 June, 1994, Bergen, Norway, 2258: 735-746.

Shapiro DB, Maestre MF, McClain WM, Hull PG, Shi Y, Quinby-Hunt MS, Hearst JE, Hunt AJ. Determination of the average orientation of DNA in the octopus sperm *Eledone cirrhosa* using polarized light scattering. *Applied Optics* 1994:33; 5733-5744.

Shapiro DB, Hull PG, Shi Y, McClain WM, Quinby-Hunt MS, Maestre MF, Hearst JE, Hunt AJ. Towards a working theory of polarized light scattering from helices. *J. Chem. Phys.* 1994; 100; 146-157.

Shapiro DB, Quinby-Hunt MS, Hearst JE, Hull PG, Hunt AJ. Light Scattering from Marine Dinoflagellates: Single Particle Systems and Ensembles, submitted to *J. Geophys. Res.* 1994.

New Approaches to Assessing the Oceans as a Carbon Sink

G.R. Dickens and M.S .Quinby-Hunt

The world's oceans cover approximately 70% of the surface of the earth. The ocean provides sources and sinks for CO_2, CH_4, and other gases important to the global carbon budget. The importance of oceanic biogeochemical processes in the global carbon budget is clear, but many uncertainties remain. A better understanding of the ocean's carbon budget is essential for understanding the mechanisms and kinetics of climate control.

Oceanic phytoplankton are an important component of the global carbon budget. They consume CO_2 and may release it to the water column when they decompose. After death, phytoplankton and other marine organisms decompose in the water column consuming oxygen and releasing CO_2; in regions of high productivity or low oxygen, oceanic biomass falls to the bottom and is buried in the sediments. Oxidation of biomass may cause parts of the water column and sediments to become anoxic. After the detritus has consumed all oxygen and sulfates, microbial and thermodynamic processes may cause formation of methane from the detritus.

Methane formed from the decomposition of phytoplankton is an important carbon sink. After formation, methane may be sequestered in hydrates (clathrates). Clathrate hydrates are solids in which water forms a rigid lattice of cages that may contain a guest molecule. In the marine environment, the guest molecule is often methane, carbon dioxide or hydrogen sulfide (all formed during phytoplanktonic decomposition). The existence of large regions of methane clathrates on the ocean floor has been suggested based on interpretation of acoustic records: estimates report that on the order of 10^{19} g of methane exist in hydrates globally. Methane and carbon dioxide clathrates have been recovered in the Deep Sea Drilling Project and other marine sediment cores. Clathrates can be present in marine sediments under water column depths as shallow as 70 m under cold-water conditions. Because gas hydrates form only at certain pressures and temperatures, they may be destabilized due to warming of bottom waters or changes in sea level and thereby released to the atmosphere. A significant increase in CH_4 over historical levels has been reported under sea ice off Alaska. The fate of the methane formed in the sediments may impact geochemical climate regulatory mechanisms.

The thermodynamics and kinetics of clathrate formation under highly reducing marine conditions are not well understood. As the extent of marine clathrates may be great, an increased precision in the estimates of their extent would enable refinements of carbon budget models and allow better predictions of the potential impacts of clathrates on global climate regulation, their potential as fossil fuels,

and the possibility that they present geological hazards.

A study of the conditions of methane clathrate formation under marine conditions is continuing at LBL. Preliminary experiments conducted using deaerated distilled water and commercial methane and carbon dioxide demonstrated our ability to duplicate results from other researchers. The CO_2 clathrates were found to be polycrystalline, white (similar in appearance to dry ice) and could be described as effervescent ice. Methane clathrates formed at higher pressures (~1200 psi) and at similar temperatures. The material retrieved was multicrystalline and the vapor released as the clathrate evaporated could be ignited.

The thermodynamics and kinetics of marine gas hydrates have generally been studied in distilled water and in the presence of oxygen. We have measured methane hydrate stability conditions in sea water (salinity = 35 parts per thousand). For the pressure range of 2.75-10.0 MPA, at any given pressure, the dissociation temperature of methane hydrate is depressed by approximately -1.1°C ["minus one point one degrees calcius"] relative to the pure methane-pure water system. The experimental results are consistent with previously reported statistical thermodynamic predictions and provide a minimum constraint concerning the depth ranges over which methane is stable in the marine environment.

Pressure and temperature conditions of methane hydrate dissociation were determined for 13 solutions containing variable concentrations of Cl^-, SO_4^{2-}, Br^-, Na^+, K^+, Ca^{2+}, Mg^{2+}, NH_4^+, and Cu^{2+}. Methane-hydrate stability curves for all solutions can be successfully predicted to within analytical precision through calculating the activity of water for any solution. Using this approach and dissolved ion concentrations for pore waters in and near hydrated sediment (but undiluted by dissociated hydrate), we find that methane hydrate is slightly less stable in most pore waters than in sea water—typically -1.2 to -1.4°C at any given pressure relative to that of the methane-pure water system.

References

Dickens GR, Quinby-Hunt MS. Methane hydrate stability in seawater. *Geophysical Research Letters* 1994: 21; 2115-2118.

Dickens GR, Quinby-Hunt MS. Methane hydrate stability in pore waters. Submitted to 1994 Fall Meeting of the American Geophysical Union, San Francisco, CA, December 5-9, 1994.

Lawrence Berkeley Laboratory Interests, Approaches, and Capabilities in Ecological Research on the Consequences of Climate and Atmospheric Change

M.S. Quinby-Hunt, N.J. Brown, S. Jovanovich

Compelling evidence supports the idea that human activities have changed atmospheric composition and ecosystems. Less certain is the impact of these changes, their interrelationships, and their significance for a sustainable future. The types of changes that have been predicted are startling: an average temperature increase of 1.5°- 4.5°C by 2025 to 2050 accompanied by an average sea level increase of 0.3-0.5 m. Incidences of extreme weather events are predicted to be more frequent. The warming signal is expected to be more pronounced at high latitudes. The interaction of climate changes with ecosystems is not understood, yet changes in ecological systems have significant economic consequences. For example, the importance of agriculture to the California economy is indicated by annual marketing receipts of over $15 billion. Understanding the risks and the time frames of climate change is crucially important for optimizing planning required to sustain development.

The interaction of terrestrial ecosystems with climate is complex containing multiple higher level effects and feedback loops. The Program for Ecosystem Research in the Office of Health and Environmental Research of the U.S. Department of Energy (DOE) requested that the DOE National Laboratories provide new innovative approaches and strategies to identify and quantify the vulnerability of ecological systems to atmospheric and climatic changes. These new approaches and strategies were to (1) develop and improve our predictive understanding of how the biosphere responds to atmospheric, climate, and land use changes and (2) determine feedback effects of the biosphere on the atmosphere and climate. Further, the laboratories were to identify unique scientific capabilities applicable to the problem and to discuss the collective capabilities of the DOE laboratories, identify non-DOE researchers and capabilities, and discuss the advantages and disadvantages of having the DOE laboratories participate in the development of coordinated multi-laboratory proposals.

New Approaches and Strategies

Prediction of ecosystem alterations and responses to changes in climate and atmospheric composition requires understanding how the biosphere at local, regional, and global scales reacts to these changes. LBL devised the following approaches and ideas to provide information critical to understanding, modeling, and predicting the consequences of global change on the biosphere. Currently, LBL has ongoing research supported by DOE and other Federal agencies in each of the focus areas. This research could benefit from more resources, collaborations, and integration.

Adaptive and Molecular Genetic Responses: Studies of the Interactions of Ecosystems with Climatic and Atmospheric Changes

To predict, mitigate, or accommodate the effects of climate and atmospheric change, it is essential to investigate and understand both the initial effect on ecosystems and the consequences of the ecosystem response. Three processes with the potential for large impacts on feedback between ecosystem and climate are carbon cycling, albedo, and transpiration. Measurement of ecosystem impacts and feedback mechanisms is essential at field-scale to provide a basis for eventual extrapolation to local, regional, and global scales. LBL and the University of California at Berkeley are currently collaborating on an integrated study of the ecology and gas fluxes of a pristine alpine meadow. This meadow is representative of a number of geographically extensive ecosystems that are at relatively high latitude and are high in carbon content. Changes in these ecosystems are expected to have a significant effect on carbon cycling and global albedo.

Recent developments in molecular genetics enable development of markers of genetic change. These may be useful in predicting the vulnerability of that

ecosystem to change in subsequent generations. This concept could be tested in the same field experiments used to elucidate the interaction between ecosystems and climate. To develop both an understanding of feedback between ecosystems and climate as well as diagnostic tools that may be useful in predicting impending change in ecosystems, a variety of adaptive responses to stressors such as desiccation and warming should be examined. Their impact on alterations in key processes such as carbon cycling should be determined. This research could be extended to additional sites, which would provide necessary information about variability and scalability. The investigation would augment our ability for broad-scale prediction of patterns of ecological change that could be used to develop more accurate predictions of feedbacks between ecological response and climate change.

Anoxic Regimes, Environmental Stress, and Greenhouse Gas Biogenesis

Oceanic temperature increase and sea level rise will enhance algal growth and increase the intensity and extent of hypoxic and anoxic zones in coastal zones. These changes could kill large numbers of organisms including fish and shellfish, cause dramatic changes in species composition and diversity in coastal marine ecosystems, and disrupt local land use. Areas at risk of increased anoxia should be identified and sufficient information gathered for each area on resident population, land use, and climatological and geological descriptions to permit assessment of the potential impacts.

In addition to increased anoxia, sea-level rise may also submerge coastal lands, including wetlands, low-lying agricultural lands, and coastal human communities. This submersion, in addition to consequences to inundated communities, will alter coastal habitats and therefore modify species composition. Moreover, it could cause chronic or episodic toxicity or enrichment to affected ecosystems. Increased temperatures will be advantageous for some invading species, further stressing indigenous species that will be simultaneously attempting to adapt to environmental changes. Both these factors and the anoxic potential may synergistically magnify the disruption of coastal ecosystems. The extent and impact of these mechanisms should be investigated. If the coastal regions potentially impacted by increased anoxia and chronic or episodic sources of toxicity/enrichment are identified and the extent and mechanisms of impact are characterized, lead times required for intervention and possible mitigating strategies can be determined.

Changes in species composition due to spreading anoxia may result in increased production of greenhouse gases (*e.g.*, methane, carbon dioxide, nitrous oxide) and exacerbate warming trends. The extent and impact of greenhouse-gas release associated with changing bacterial communities should be determined and used to predict climate changes. Exploratory research indicates that biogenic marine gas hydrates (clathrates) store a vast quantity of carbon as methane that also may be released. Because the quantity of carbon stored in clathrates is large but uncertain, a better definition of their extent, mechanisms of their formation, and their role in climate regulation is essential to understanding and predicting their potential effect on atmospheric composition and climate.

Integrated Paleoclimatic and Paleoecological Study of a Western Delta Watershed

The interaction between past global climate changes and terrestrial ecosystems are encoded in the geological-record via layered deposits that contain a host of isotopic, chemical, and biological indicators of past climates. An integrated investigation of paleoclimatic and paleoecologic records at a single, coastal delta locality, for example the San Francisco Bay/San Joaquin-Sacramento River Delta, and the surrounding region, should be conducted to determine the past consequences of global climate change. This study would enable more accurate forecasting of the ecological consequences of current climatic trends. This will be particularly useful for advancing model development. This study will provide critical information necessary to sustain California's development while it is impacted by climate change. Moreover, the historical record will provide essential data for model validation.

To predict future ecological changes from climatic and atmospheric changes, an understanding is required of past biological changes and the crucial factors that caused these changes. Potential invaders and species at risk of extinction must be identified, since they will determine the course of change for ecosystems. In addition to applying well-developed methods to determining past climates, promising new techniques should also be developed. Determining climate change in conjunction with an examination of the consequential changes in biological communities provides a better understanding of the feedback functions involved and their timing.

Interactions Between Biogenic and Biomass-Derived Aerosols and Climate

Albedo change is a marker of ecological system/climate change feedback that could be characterized by measuring the optical properties of different plant communities and atmospheric aerosols. Plant communities form a large carbon reservoir and are significant contributors to local albedo. Alterations in albedo are important because changes in the optical properties of the Earth's surface may cause warming or cooling. Plant communities are affected by and alter the physics and chemistry of the atmosphere. Local, regional, and global climate change and ecosystem compositions interact via complex feedback mechanisms that affect the quantity of carbon stored and the global albedo. Changes in plant emissions, heat and moisture flux changes, and incidence of drought and extreme events stimulate the feedback between terrestrial ecosystems and the climate. Alterations of the species composition or the presence of stressed plants change the heat transfer characteristics of the canopy. The effects of the changes on the albedo of the canopy and the climate below it should be examined.

Increased incidence of drought and extreme events may enhance the possibility of wide-spread fires. The combustion products of these fires will alter local and potentially regional and global albedo. Characteristics of combustion processes determine the type and concentration of combustion products distributed in the atmosphere. The optical properties of particulate combustion products and particles formed from combustion-generated precursors need to be measured to determine albedo. To understand, predict, and mitigate the effects of global climate change on terrestrial ecosystems and the resultant feedback, the effect that plant communities have on local environments and the change that might be expected with varying climate must be investigated and quantified.

International Assessment of Ecological Consequences of Climate Change on Forest Sectors

Forest ecological systems are large carbon reservoirs that are important for the global economy and for climate regulation. Forests support great biodiversity. They also contribute greatly to the pristine and aesthetic character of the environment. Data on vulnerable forested ecosystems should be gathered to identify the extent of their vulnerability. Data collection should be conducted in concert with experts and scientists from affected locales. This investigation complements satellite data, because it permits groundtruthing and provides crucial information not available from remote sensing or in the published literature. Methods and models suitable for analysis of the data should be developed and/or adapted. Candidate variables are nutrient cycling, greenhouse-gas fluxes, ecosystem health, yields of essential products, and potential changes in trade patterns associated with such ecosystem changes. Data should be compared and analyzed across countries and time periods. Global trade models should be adapted and used to study the implied trading implications of climate and atmospheric changes on forested ecosystems. This research will provide policy makers information on the forest ecosystems at risk, allow estimation of the rates of changes in forest sectors, and allow them to develop and assess mitigating strategies, as well as adaptive commercial policies.

Capabilities and Facilities

LBL has a large number of unique scientific capabilities that should be used more extensively to investigate the effects of global climate change on terrestrial ecosystems and the feedback responses of those ecosystems. These could be used to support the suggested research described above. LBL's facilities and capabilities could provide excellent opportunities for future collaborations.

Collaborations

Environmental and ecological systems are inherently complex and highly variable over time and space. Long-term, multidisciplinary research that is carefully integrated would be required to develop an understanding of these systems to enable formulating sound policy decisions. The proposed research would help provide a more scientifically defensible and cost-effective basis for regulation. Research having these characteristics is ideally suited for the national laboratories. In ecological research, the national laboratories are already performing integrated multidisciplinary research that involves long-established collaborations involving university and private sector investigators in the United States and around the globe. In these efforts, the laboratories provide an organizational capability and continuity that assure that research time scales are appropriate.

Sponsors

- Director, Office of Energy Research, U.S. Department of Energy:
  Office of Basic Energy Sciences, Chemical Sciences Division
  Office of Health and Environmental Research, Environmental Sciences Division
- Pittsburgh Energy Technology Center
- Battelle Pacific Northwest Laboratory
- California Institute for Energy Efficiency
- Lawrence Livermore National Laboratory, Grant LDRD-94-LW-105
- National Aeronautics and Space Administration, Microgravity Science and Applications Division
- Office of Naval Research
- University of California, Tobacco-Related Disease Research Program, Grant RT0240
- U.S. Army Corp. of Engineers
- U.S. Department of Energy AMTEX program
- U.S. Environmental Protection Agency
- University of California/NIEHS

Energy & Environment Division
Lawrence Berkeley Laboratory
University of California
Berkeley, CA 94720